Interaction of the CMB with Astrophysical Plasma

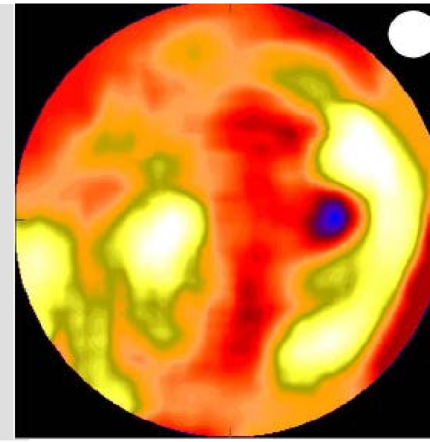

Sergio Colafrancesco
Wits University - DST/NRF SKA Research Chair
INAF-OAR
Email: Sergio.Colafrancesco@wits.ac.za

Outline

- Lecture 1
  - CMB photon interaction
  - LSS: plasma content
  - Spectral and spatial properties
  - Plasma – CMB photon interaction: basic mechanisms
  - ICS, Pair production, Primakov effect
- Lecture 2
  - The SZ effect: thermal, non-th, kinetic, polarization
  - General description
  - Galaxy clusters
  - RGs and other cases
  - Experimental outline
- Lecture 3
  - IC-CMB and high energy phenomena
  - X-rays
  - Gamma-rays
  - Multi-frequency studies
  - An experimental outline

Outline

- Lecture 1
  - CMB photon interaction
  - LSS: plasma content
  - Spectral and spatial properties
  - Plasma – CMB photon interaction: basic mechanisms
  - ICS, Pair production, Primakov effect
- Lecture 2
  - The SZ effect: thermal, non-th, kinetic, polarization
  - General description
  - Galaxy clusters
  - RGs and other cases
  - Experimental outline
- Lecture 3
  - IC-CMB and high energy phenomena
  - X-rays
  - Gamma-rays
  - Multi-frequency studies
  - An experimental outline

CMB photon interactions

γ_{CMB}-Matter interaction

Plasma target

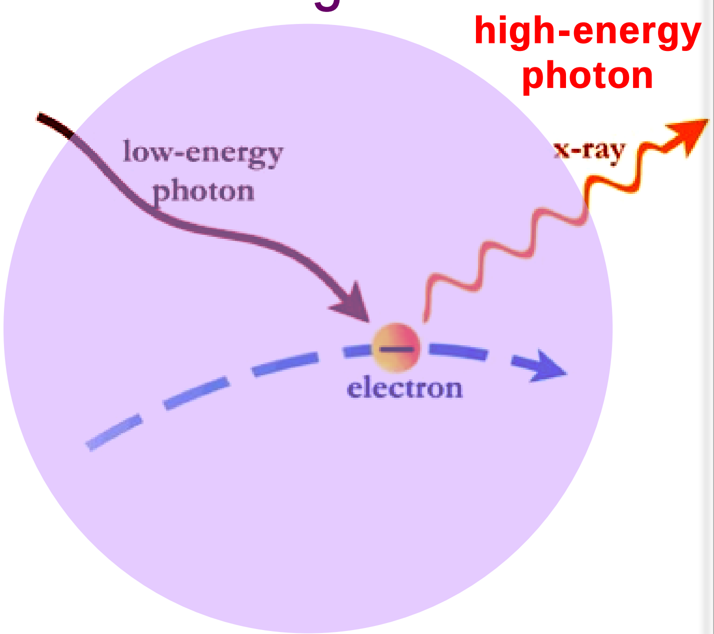

Inverse Compton Scattering
High-E electrons
- thermal (supra-thermal)
- relativistic

γ_{CMB}-Radiation interaction

Photon fields target

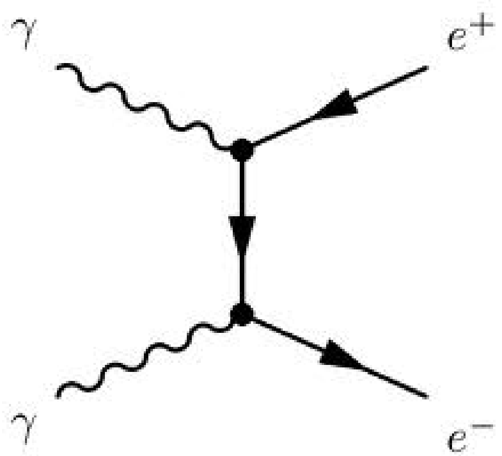

Pair production
High-E photons
- emitted by AGNs

γ_{CMB}-Field interaction

B field target

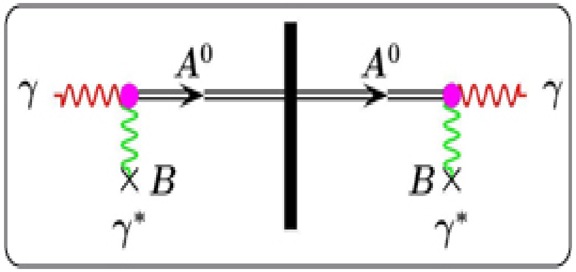

Primakov effect
Field-γ coupling
- B field (ICM, ISM, ..)

Large Scale Structures

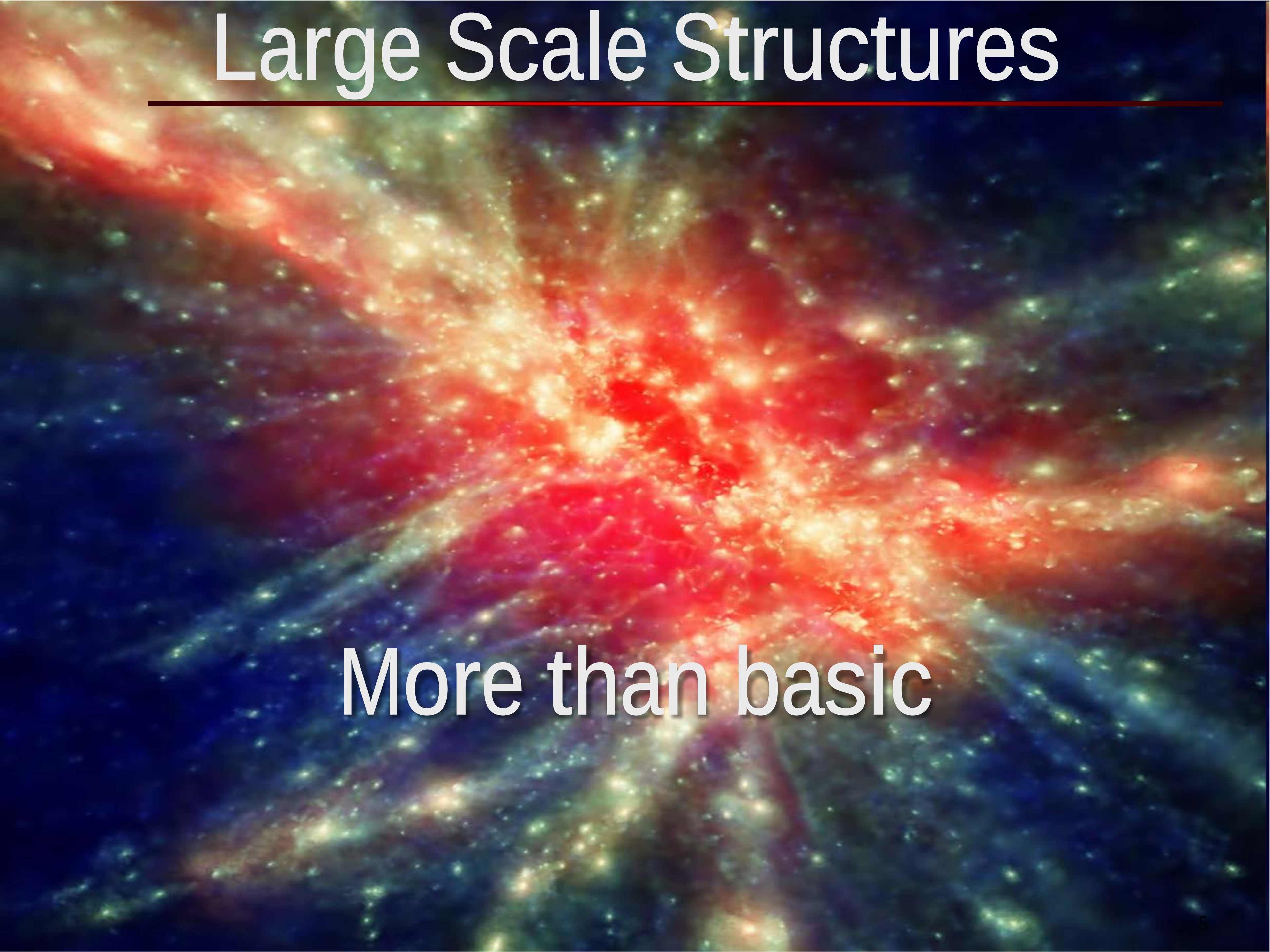

More than basic

LSS and Dark Matter

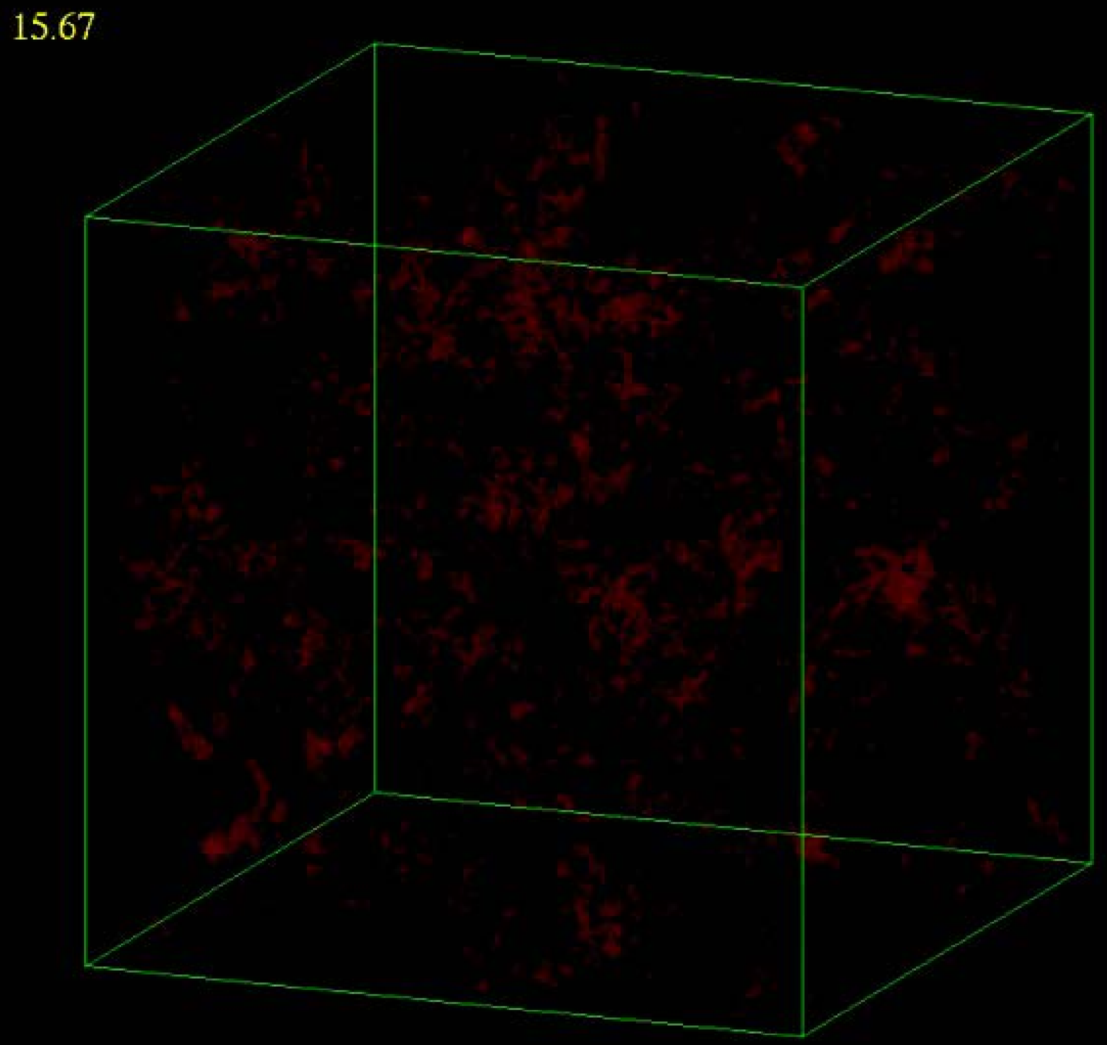

Dark Matter nature

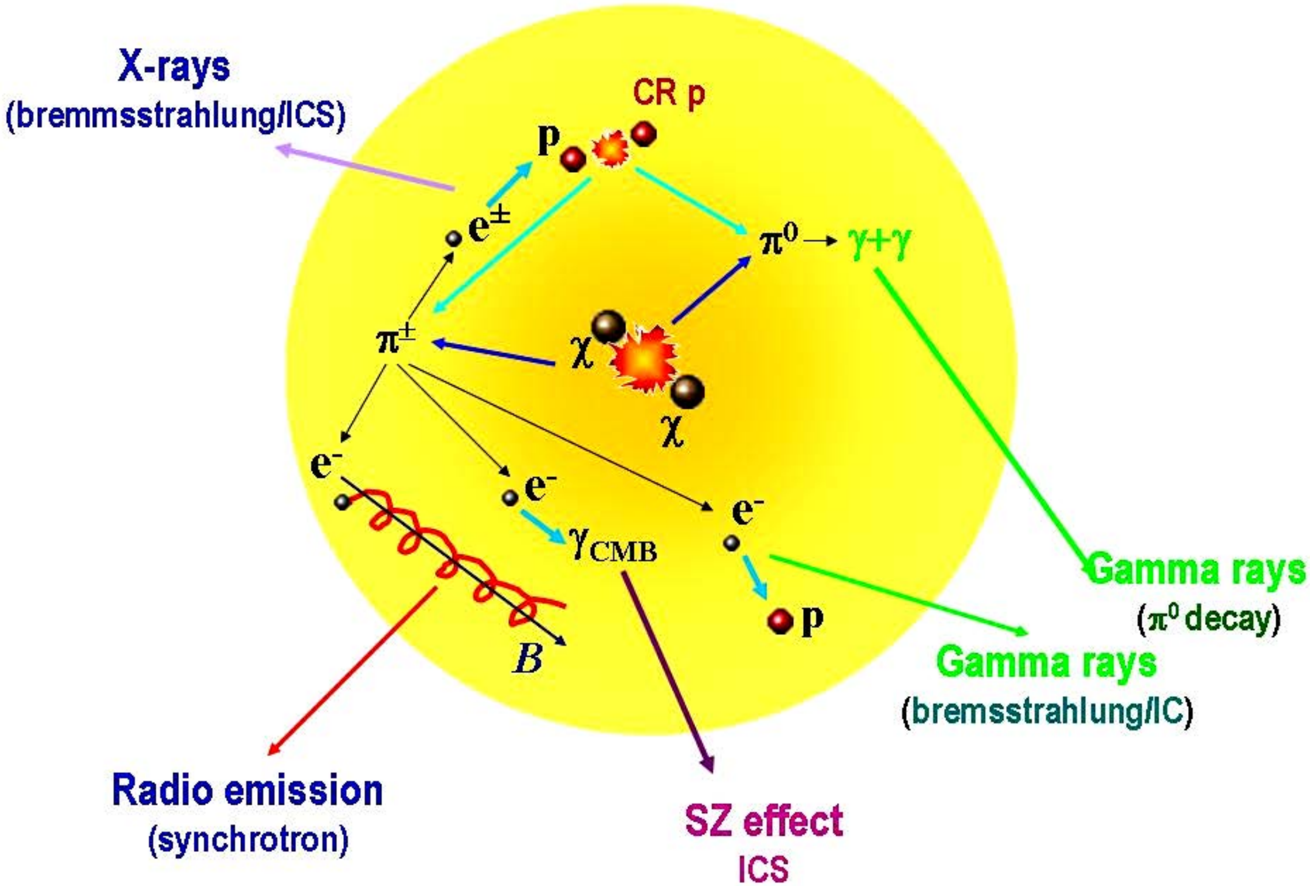

[Colafrancesco 2006, 2007]

Bullet cluster

MACS J0025.4-1222

ZwCl0024+1652

LSS shock waves

ρ_{gas}

T_{gas}

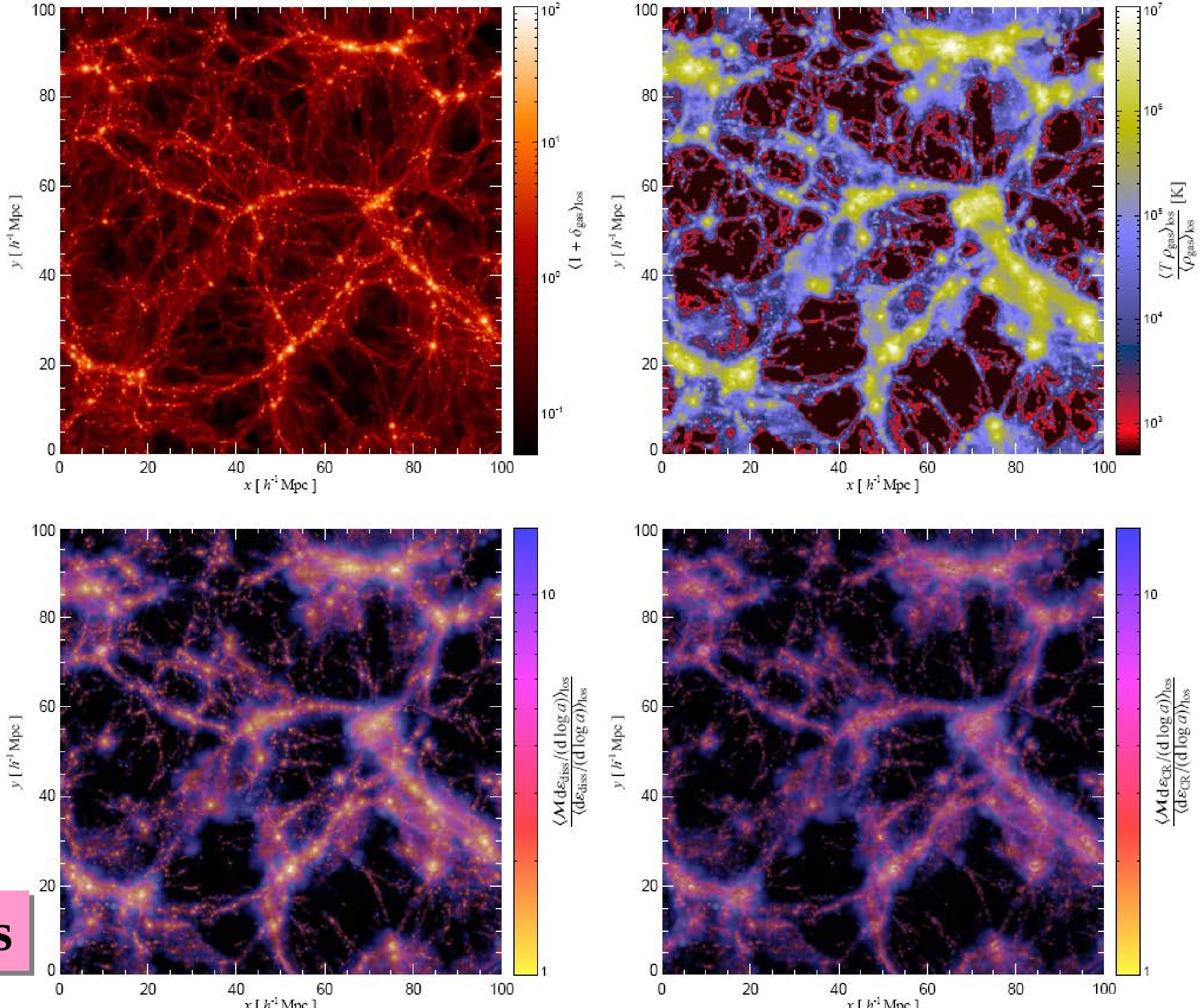

Shocks

$\mathcal{M}$

[Pfrommer et al. 2006]

LSS shock waves

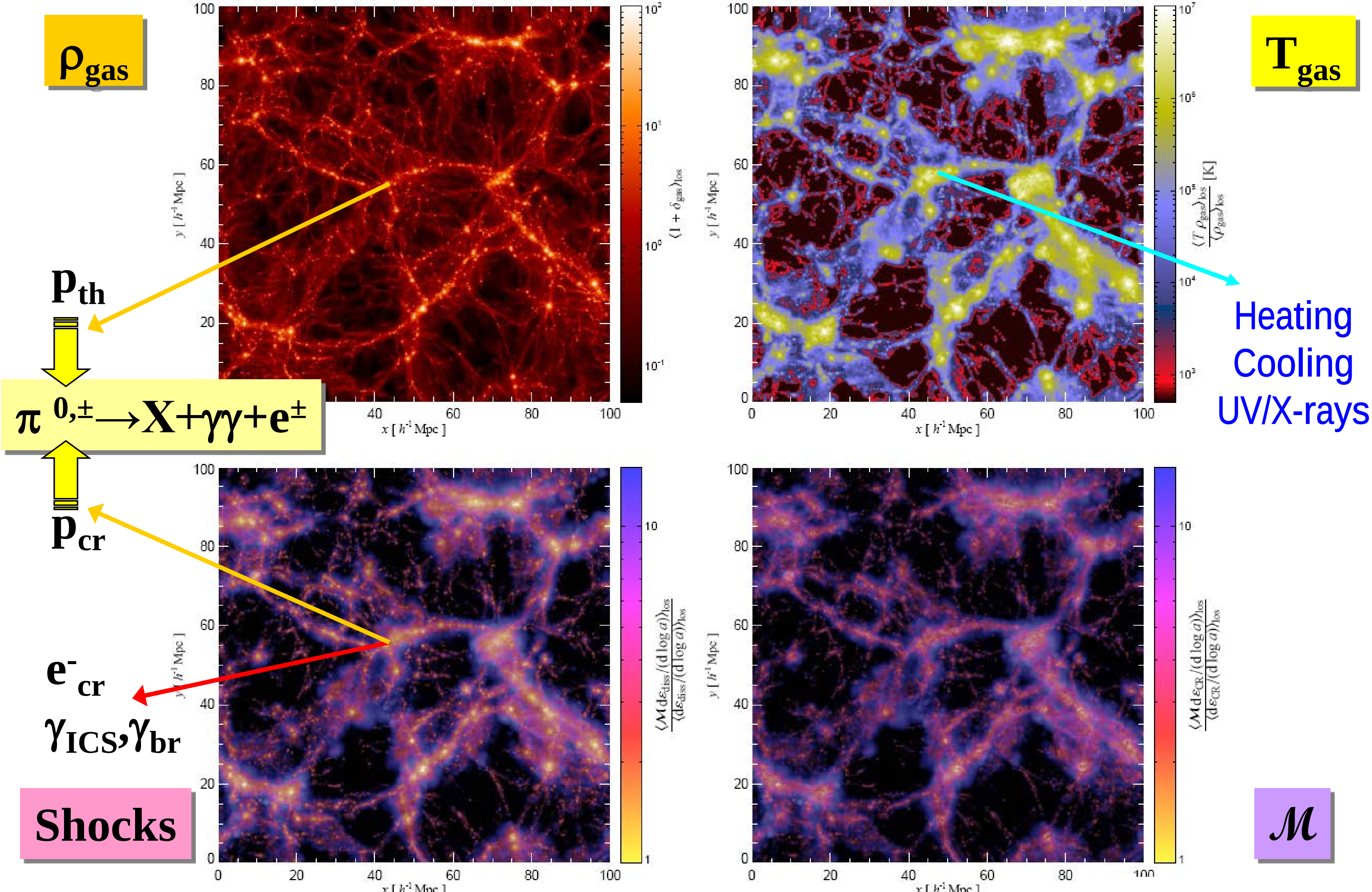

[Pfrommer et al. 2006]

Magnetic fields in LSS

Origin → Primordial / Post-recombination → G + MHD → $\mathbf{B}(\delta\rho, z; P_k)$

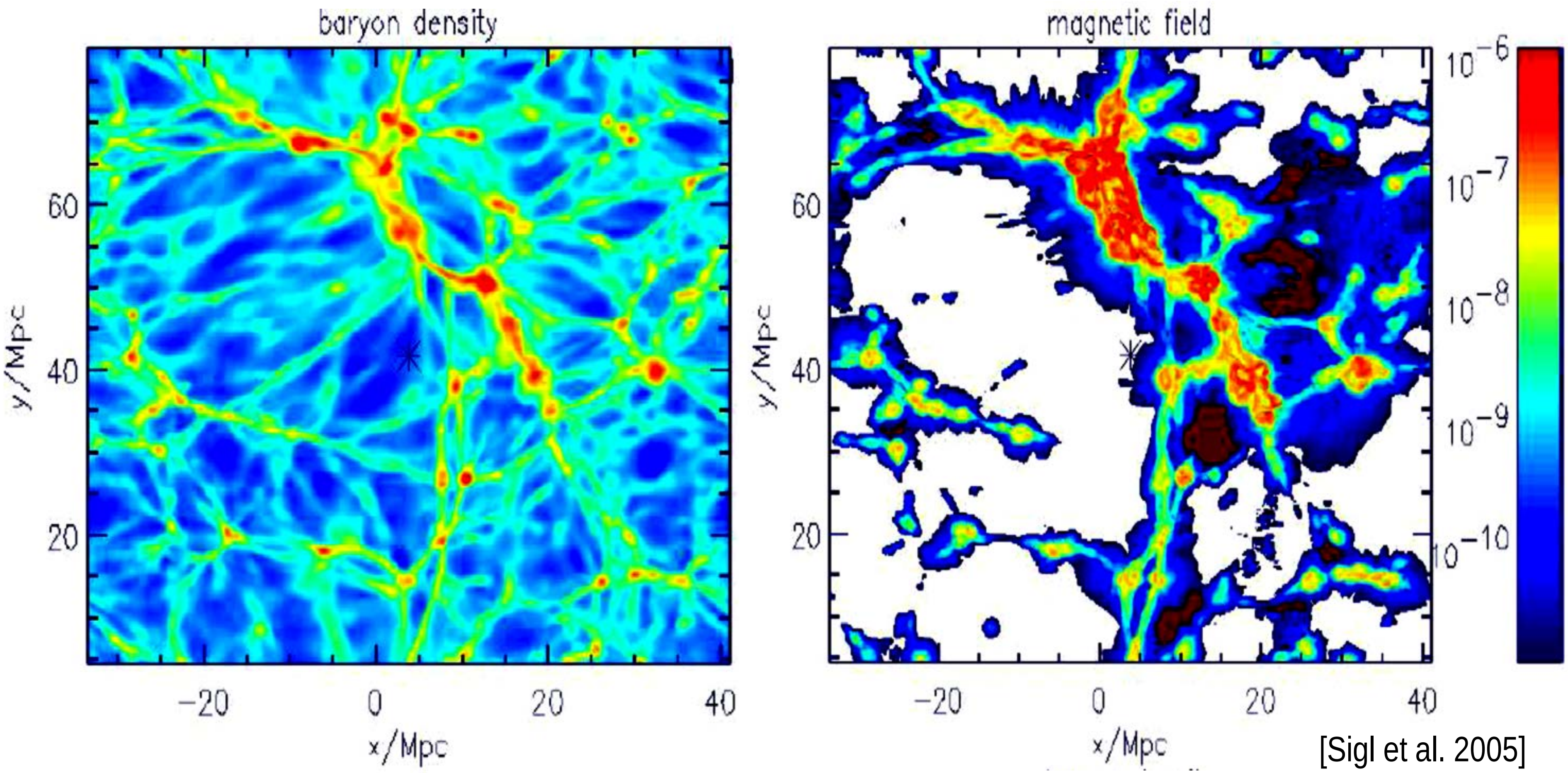

[Sigl et al. 2005]

LSS and Black Holes

One of the most massive DM clumps at t = 1 Gyr
containing one of the most massive galaxies and most massive BH

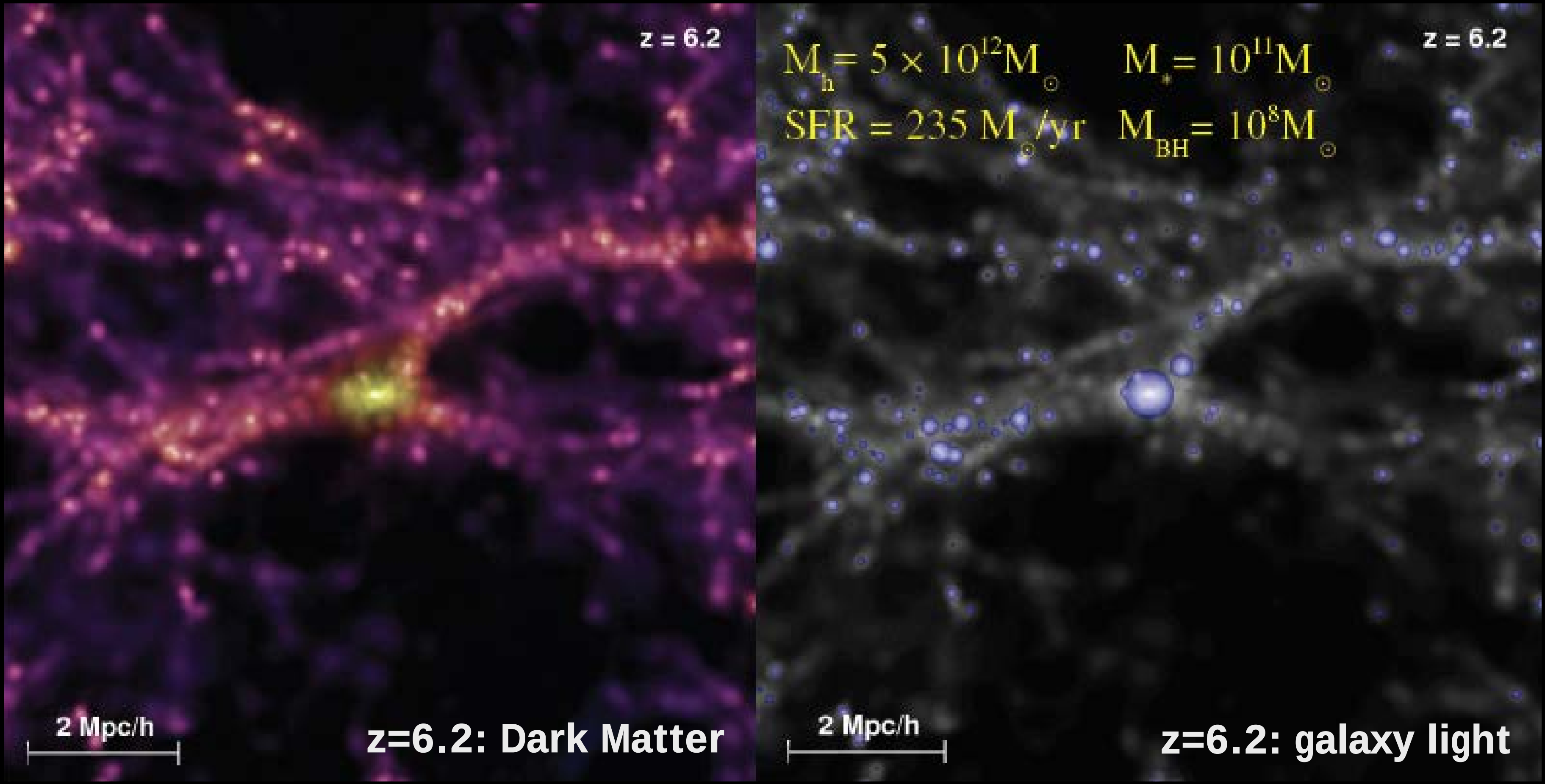

LSS and Black Holes

Sky distribution
of Blazars and RGs
at 41GHz (WMAP)

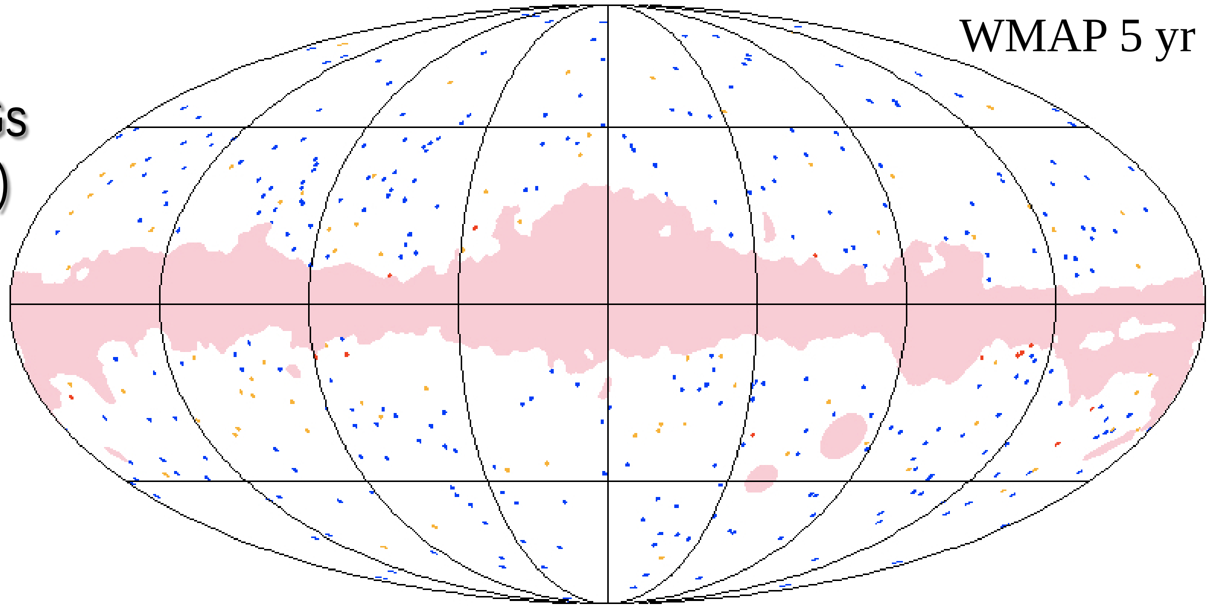

Sky distribution
of bright Blazars
at GeV energies

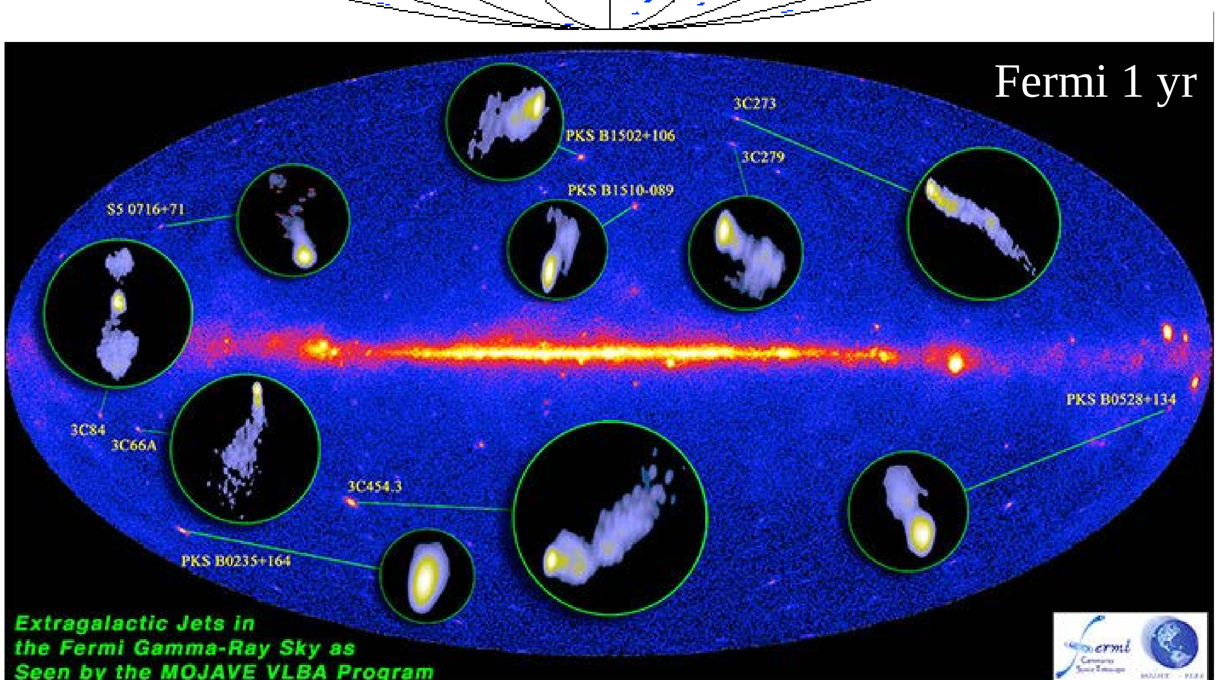

Galaxy Clusters crossroads of cosmic physics

High-E particles in clusters do exist

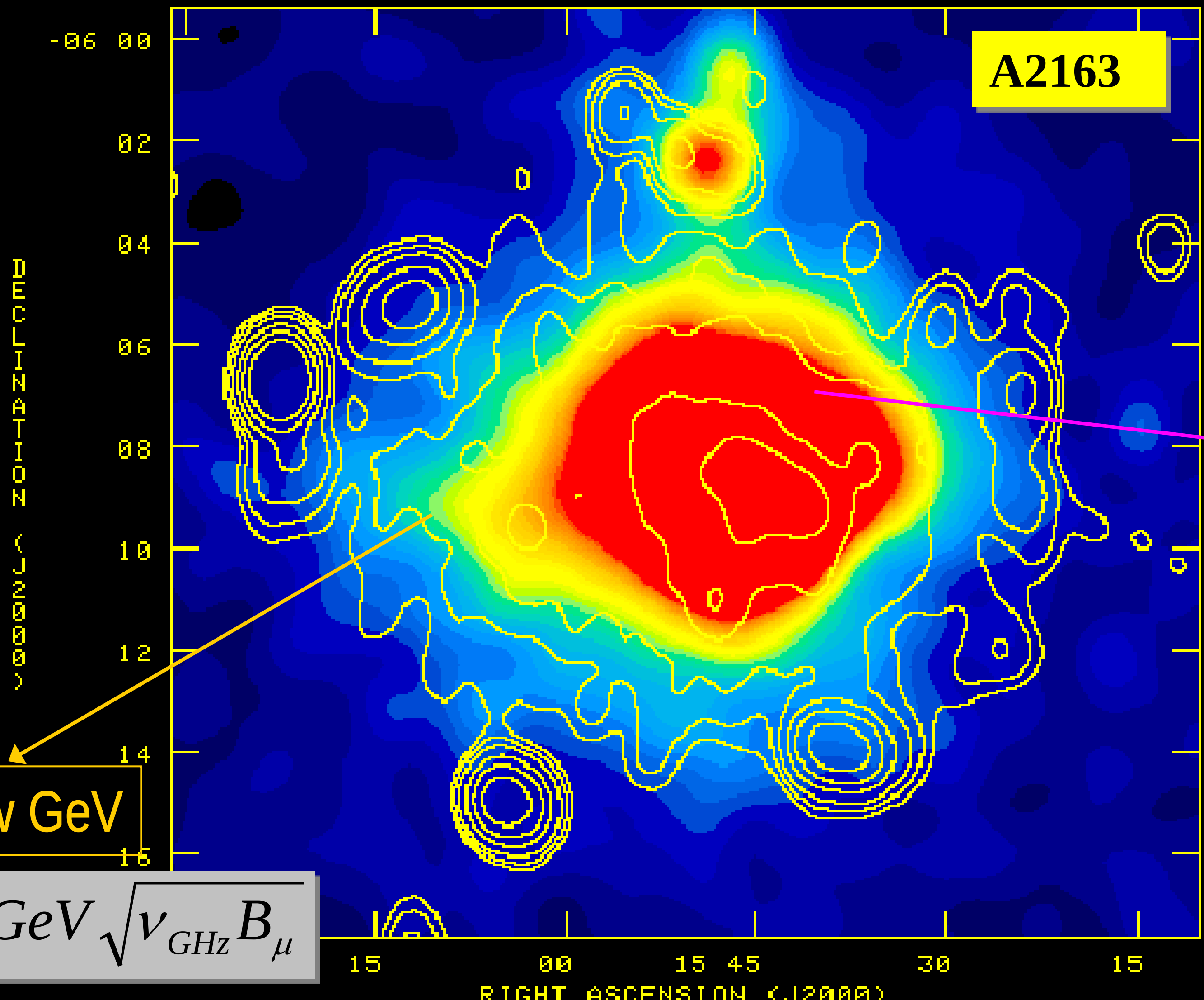

$E_e \geq$ keV

$E_e \sim$ a few GeV

$$E \approx 16.6 GeV \sqrt{\nu_{GHz} B_{\mu}}$$

[Feretti et al. 2001]

B-field in clusters: evidence

Synchrotron radiation

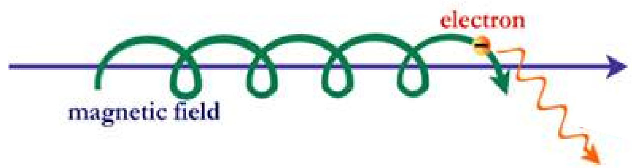

Radio Halos

$B \approx 0.1 - 5 \mu G$

Radio Relics

$B \approx 0.2 - 8 \mu G$

Faraday Rotation

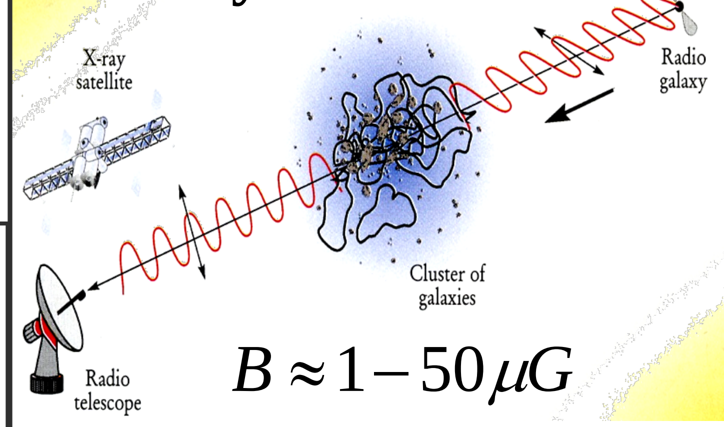

$B \approx 1 - 50 \mu G$

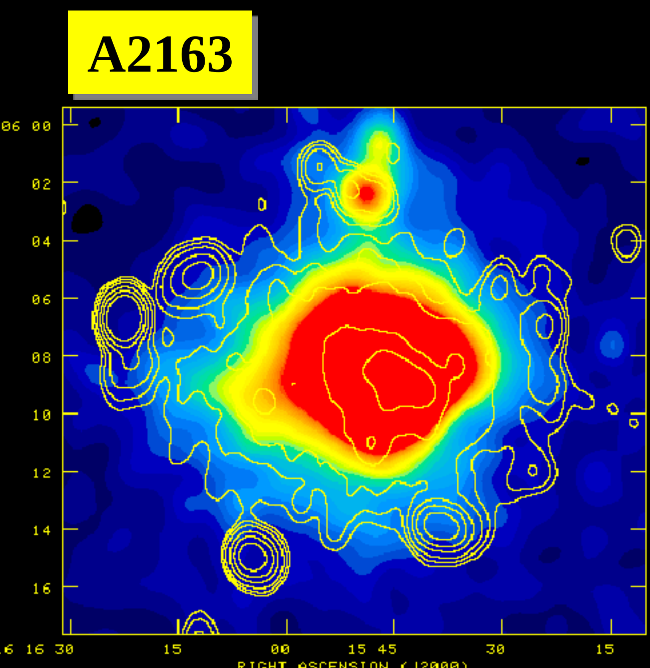

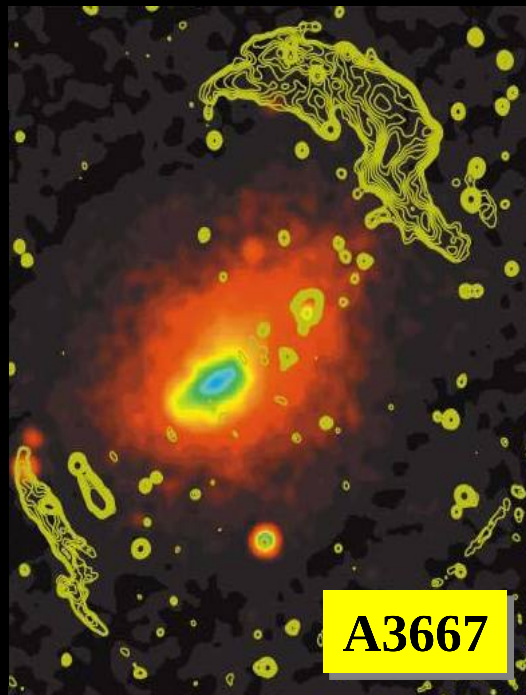

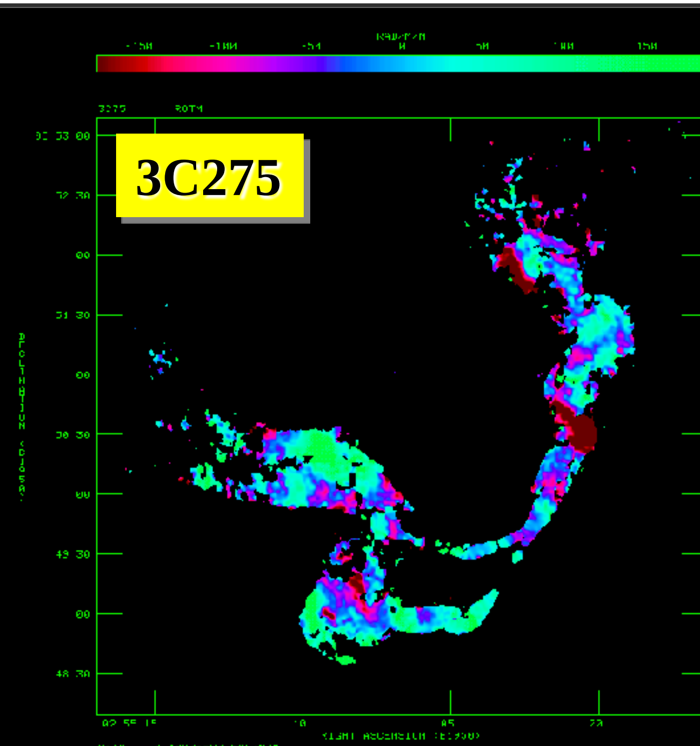

CRs in clusters: Hard X-Rays

Beppo-SAX
INTEGRAL

First detection of hard X-rays in Coma

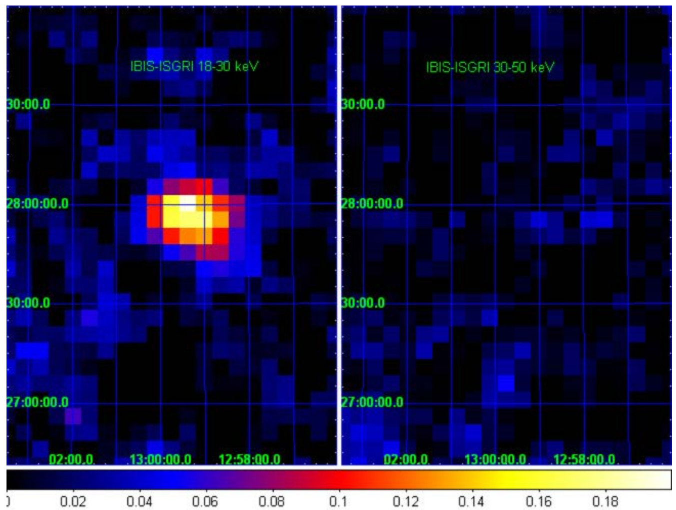

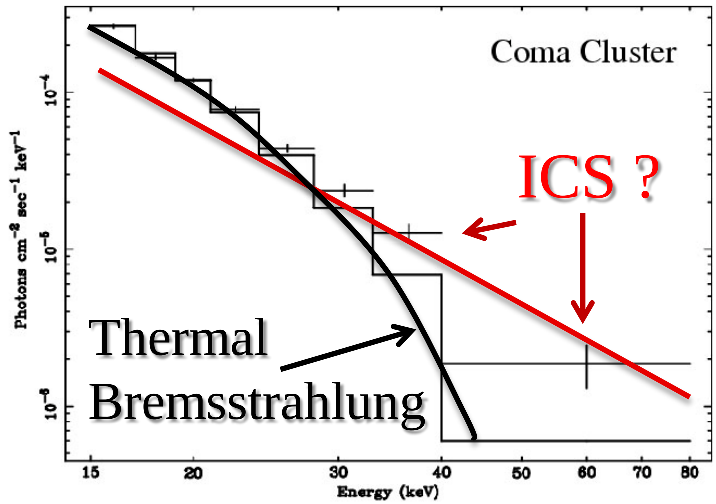

Swift-BAT

More than 20 clusters with Hard X-ray excess at E> 20 keV. Equally fit with:

- Two temperature (thermal) plasma
- Thermal plasma + non-thermal power-law

AGN emission or ICS from CR interaction ?

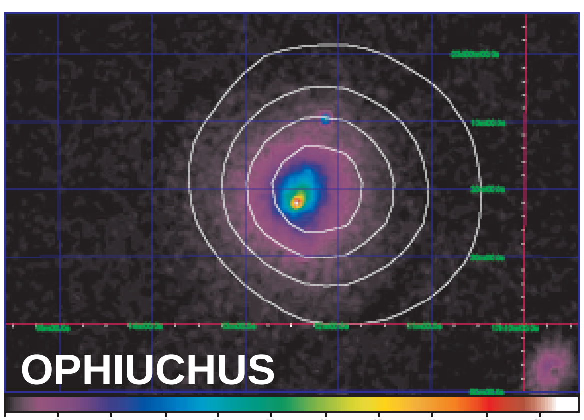

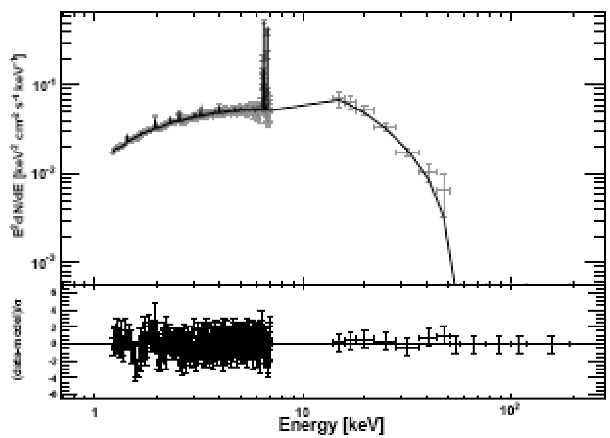

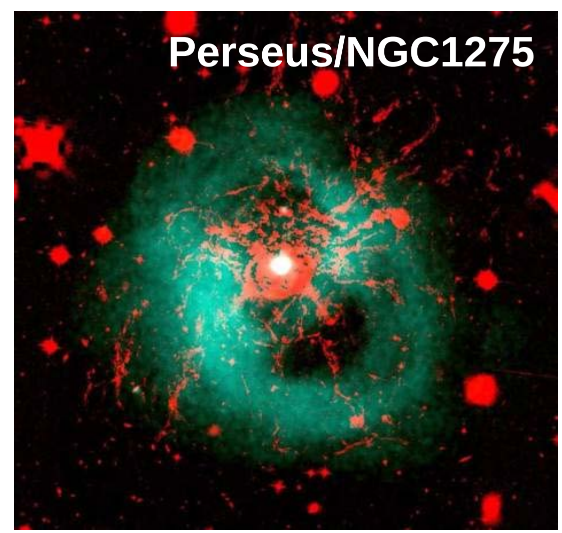

γ-rays in clusters

Only upper limits on diffuse γ-ray emission or γ-rays from RG-cluster association

The EGRET challenge

Colafrancesco (2000-1)
Scharf & Mukherjee (2002)
Totani & Kitayama (2001-2)
Colafrancesco (2002)
Reimer et al. (2002)

A1758
RG: 87GB 133050.3+504752
4 NVSS RS
Radio halo

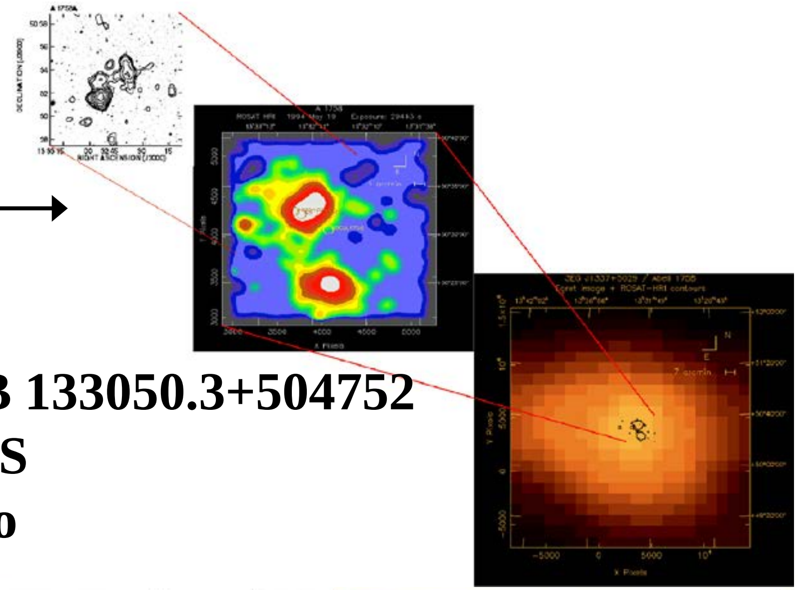

Cherenkov results

- **MAGIC**
- **HESS (2007-2008)**
  10-20 hour exp.
  No evidence
- **AUGER**

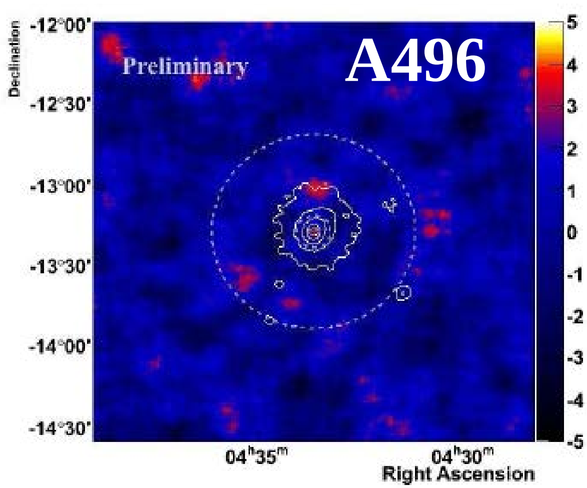

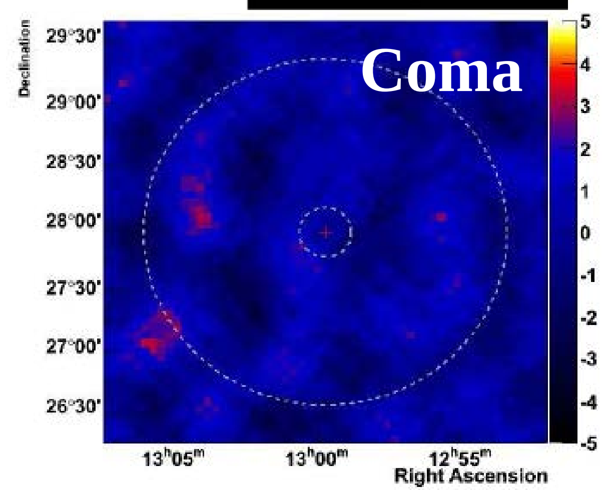

γ-rays in clusters: Fermi results

No γ-ray emission detected from galaxy clusters in 18 months LAT exposure (Aug.2008-Feb.2010)

33 clusters selected from X-ray & diffuse radio observations

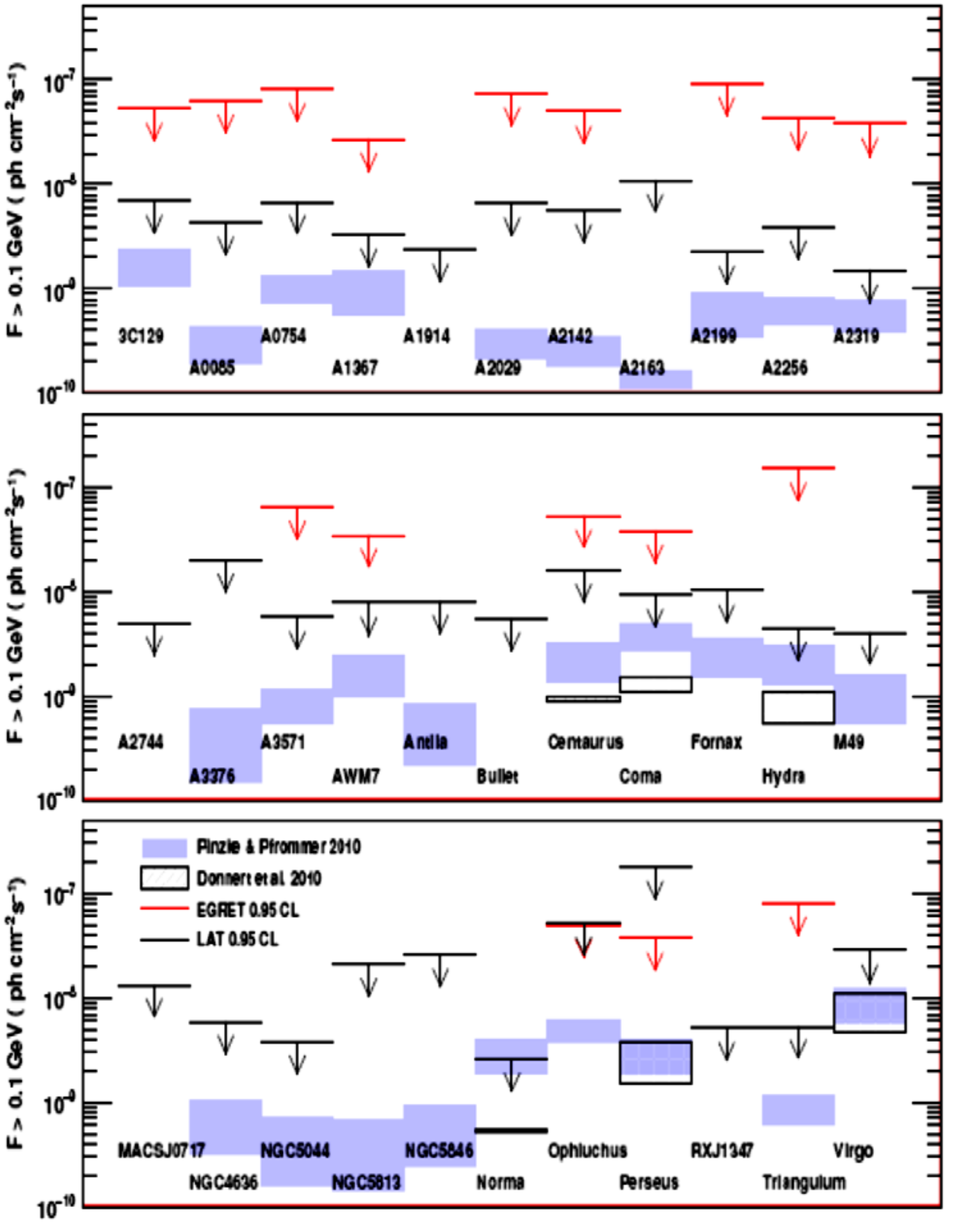

[Fermi Collaboration (Ackerman et al.2010)]

Fermi cluster detection: RG+cluster

Cluster	l (deg)	b (deg)	z	θ_{500} (deg)	θ_{core} (deg)	M_{500}/d^2 (10^9 $M_\odot$/Mpc^2)	Diffuse radio	L_X (0.1-2.4 keV) (10^{44} erg s^{-1})	T_X (keV)
X-ray flux selection									
3C129	160.43	0.14	0.0223	0.67	0.14	29.1	...	2.27	5.57
A0754	239.25	24.75	0.0528	0.40	0.05	12.8	...	3.97	9.00
A1367	234.80	73.03	0.0216	0.77	0.18	42.7	...	1.20	3.55
A2199	62.94	43.69	0.0302	0.46	0.05	12.5	...	4.20	4.28
A2256	111.10	31.74	0.0601	0.33	0.10	8.5	Halo, Relic (1, 2)	9.24	6.83
A2319	75.67	13.58	0.0564	0.37	0.05	10.9	Halo (1, 2)	16.37	8.84
A3376	246.52	-26.29	0.0455	0.36	0.17	8.5	...	2.16	4.43
A3571	316.32	28.55	0.0397	0.45	0.05	14.5	...	8.08	6.80
Antlia (S636)	272.94	19.19	0.0116	0.85	0.29	31.6	...	0.38	2.06
AWM7	146.35	-15.62	0.0172	0.85	0.10	45.0	...	2.10	3.70
Centaurus (A3526)	302.41	21.56	0.0499	1.24	0.04	87.9	...	1.19	3.69
Coma (A1656)	58.09	87.96	0.0232	0.80	0.15	49.6	Halo, Relic (1)	8.09	8.07
Fornax (S373)	236.72	-53.64	0.0046	2.01	0.36	168.1	...	0.08	1.56
Hydra (A1060)	269.63	26.51	0.0114	1.02	0.08	52.5	...	0.56	3.15
M49	286.92	70.17	0.0044	1.68	0.02	95.5	...	0.02	1.33
NGC4636	297.75	65.47	0.0037	1.27	0.02	36.3	...	0.02	0.66
NGC5044	311.23	46.10	0.0090	0.74	0.01	16.6	...	0.18	1.22
NGC5813	359.18	49.85	0.0064	1.00	0.04	28.9	...	0.02	0.76
NGC5846	0.43	48.80	0.0061	0.78	0.01	13.3	...	0.01	0.64
Norma (A3627)	325.33	-7.26	0.0163	0.89	0.18	50.2	...	3.59	5.62
Ophiuchus	0.56	9.27	0.0280	0.10	0.10	131.6	Halo (3)	12.14	10.25
Perseus (A0426)	150.58	-13.26	0.0183	0.85	0.03	49.0	...	16.39	6.42
Triangulum	324.48	-11.63	0.0510	0.42	0.06	14.7	...	12.43	9.06
Non-thermal selection									
A0085	115.05	-72.06	0.0556	0.31	0.02	...	Relic (1, 4)	9.67	6.51
A1914	67.20	67.46	0.1712	0.13	0.02	...	Halo (1, 2)	17.04	8.41
A2029	6.51	50.55	0.0767	0.25	0.01	...	Halo (3)	17.07	7.93
A2142	44.21	48.70	0.0899	0.24	0.02	...	Halo (4)	21.05	8.46
A2163	6.75	30.52	0.2010	0.12	0.03	...	Halo (1)	32.16	10.55
A2744	8.90	-81.24	0.3080	...	...	...	Halo (1)	...	...
Bullet (1E 0657-56) (a)	266.03	-21.25	0.296	...	...	...	Halo (5)	...	14
MACSJ0717.5+3745 (b)	61.89	34.02	0.546	...	...	...	Relic (6)	24.6	11.6
Other selection									
RXJ1347.5-1145 (c)	324.04	48.80	0.451	...	...	...	...	62.0	...
Virgo (M87 sub-clump) (d)	283.78	74.49	0.0036	...	0.05	...	...	...	...

Detected AGN+cl.

Detected AGN+cl.

Detected AGN+cl.

RGs at the centers of bright clusters

Cen-A clusters

NGC1275-Perseus

M87-Virgo

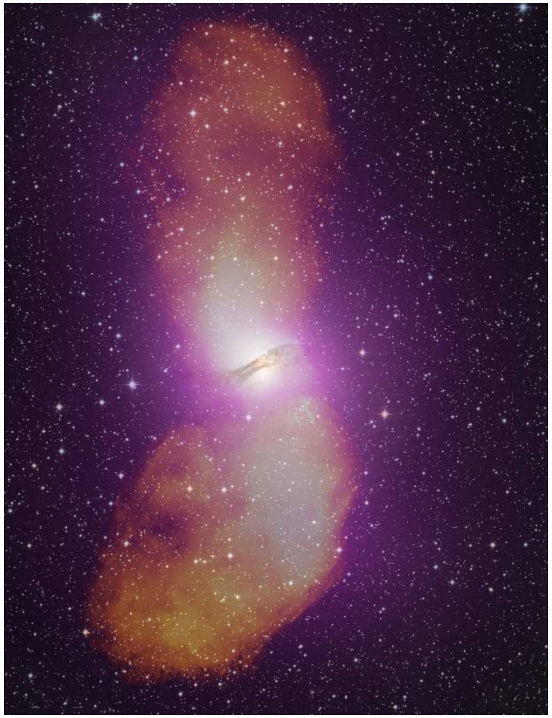

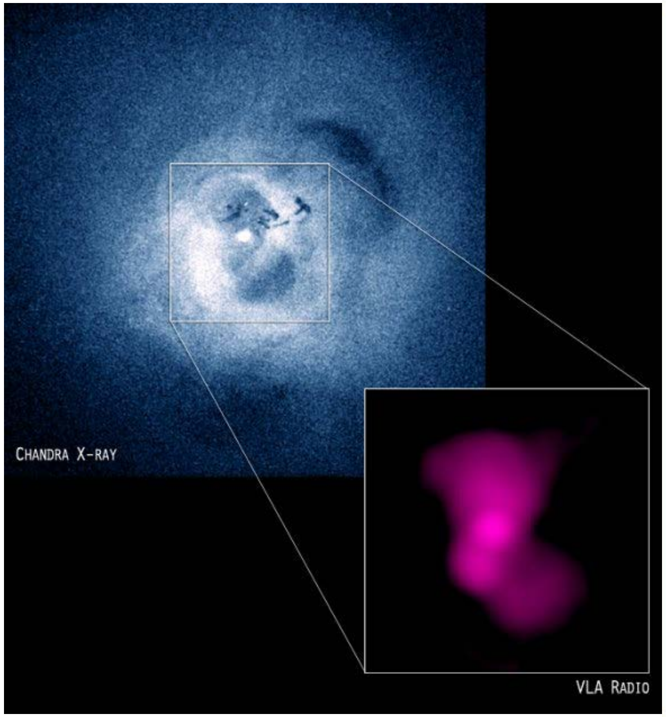

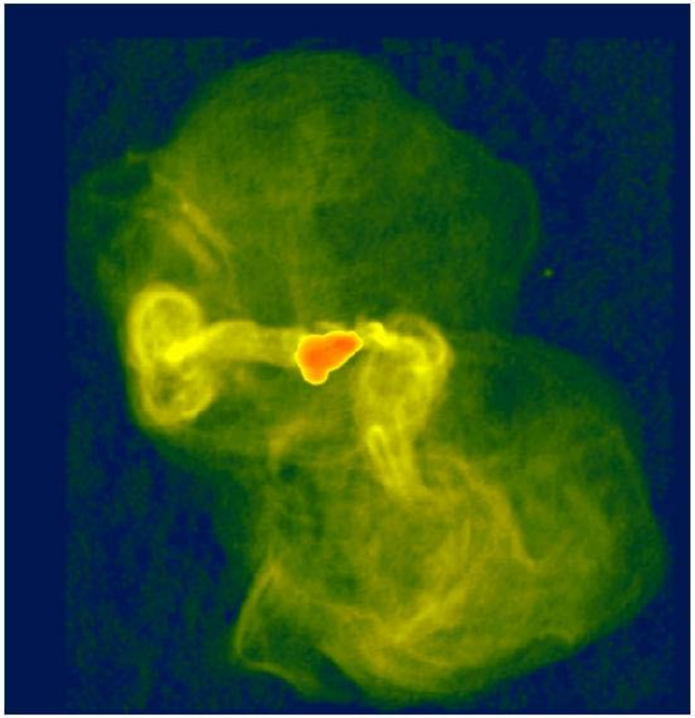

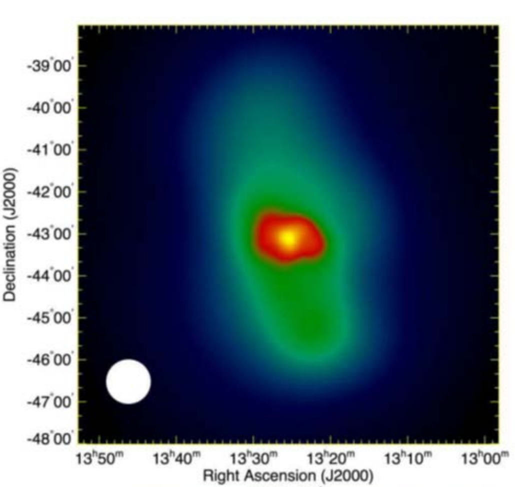

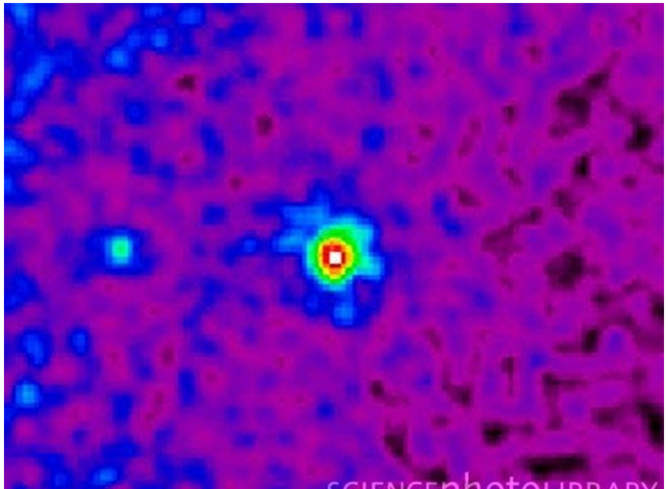

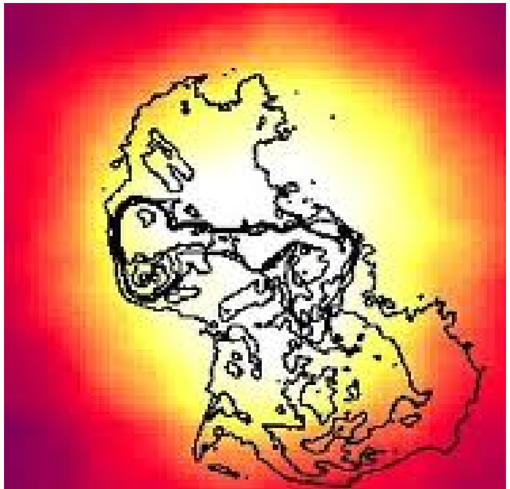

The first object descendants today

One of the most massive galaxy clusters at t = 13.7 Gyrs
The AGN descendant is part of the central massive galaxy

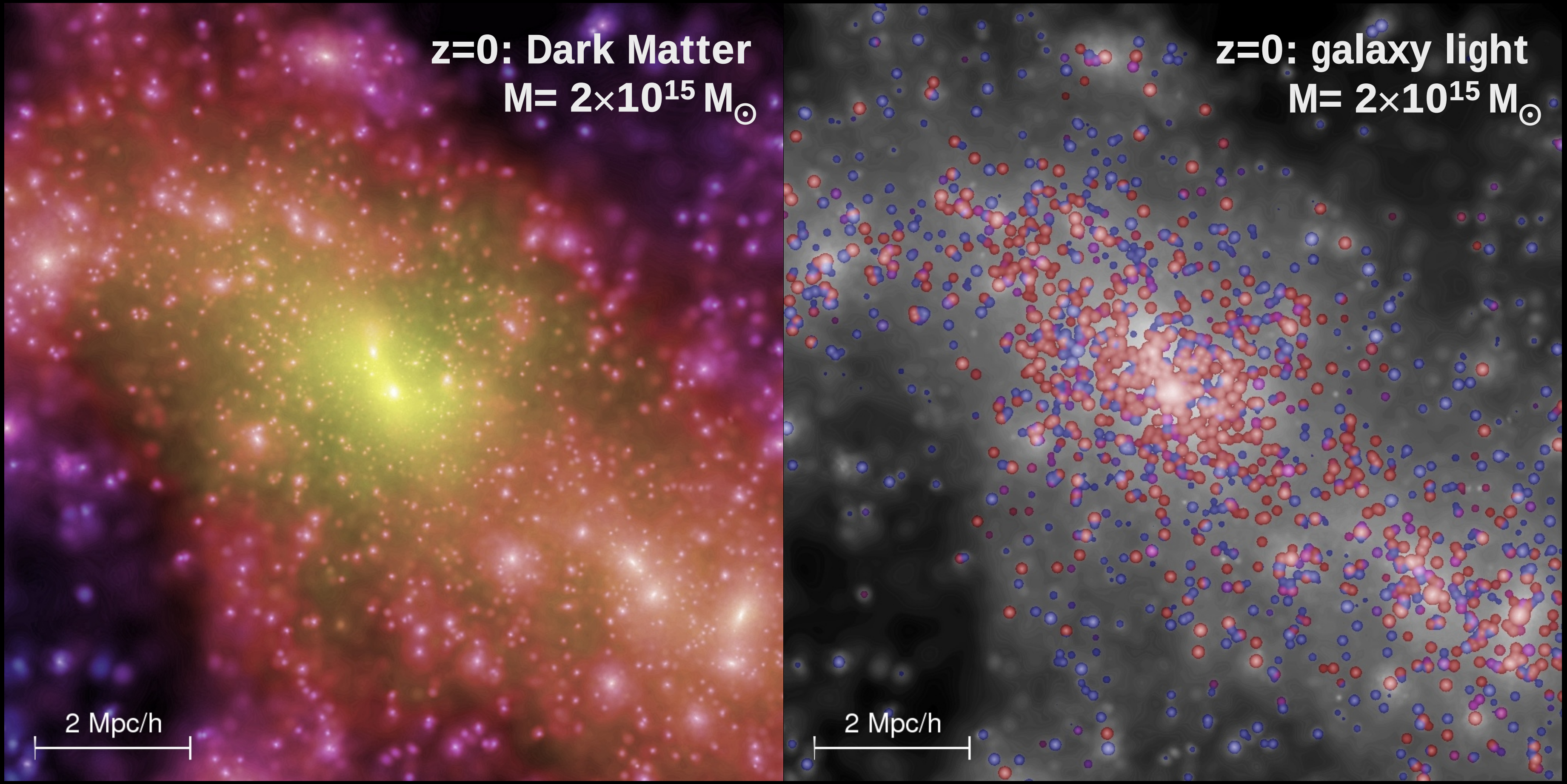

BHs in galaxy clusters: evidence

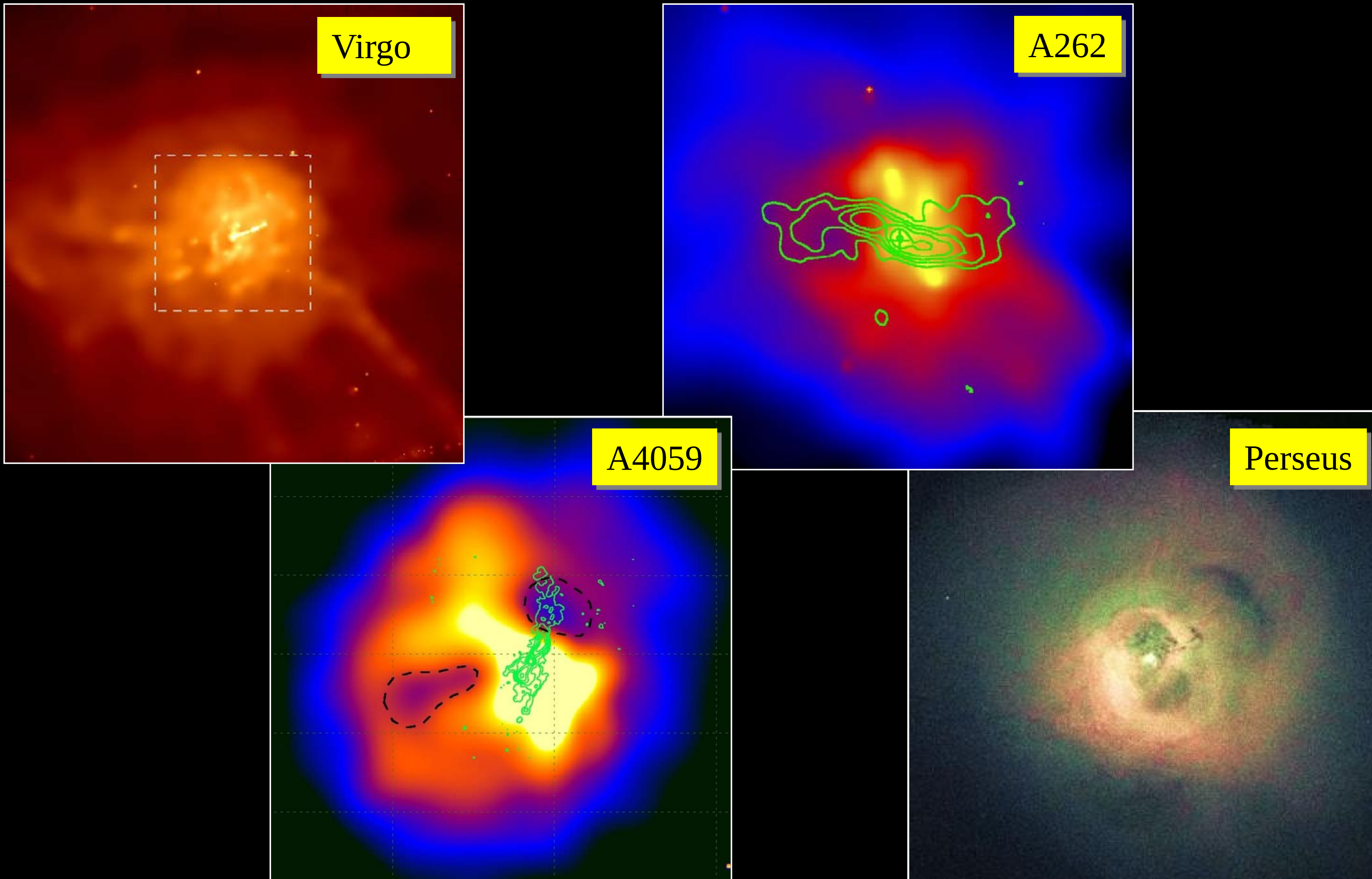

BHs: ejecta and feedback

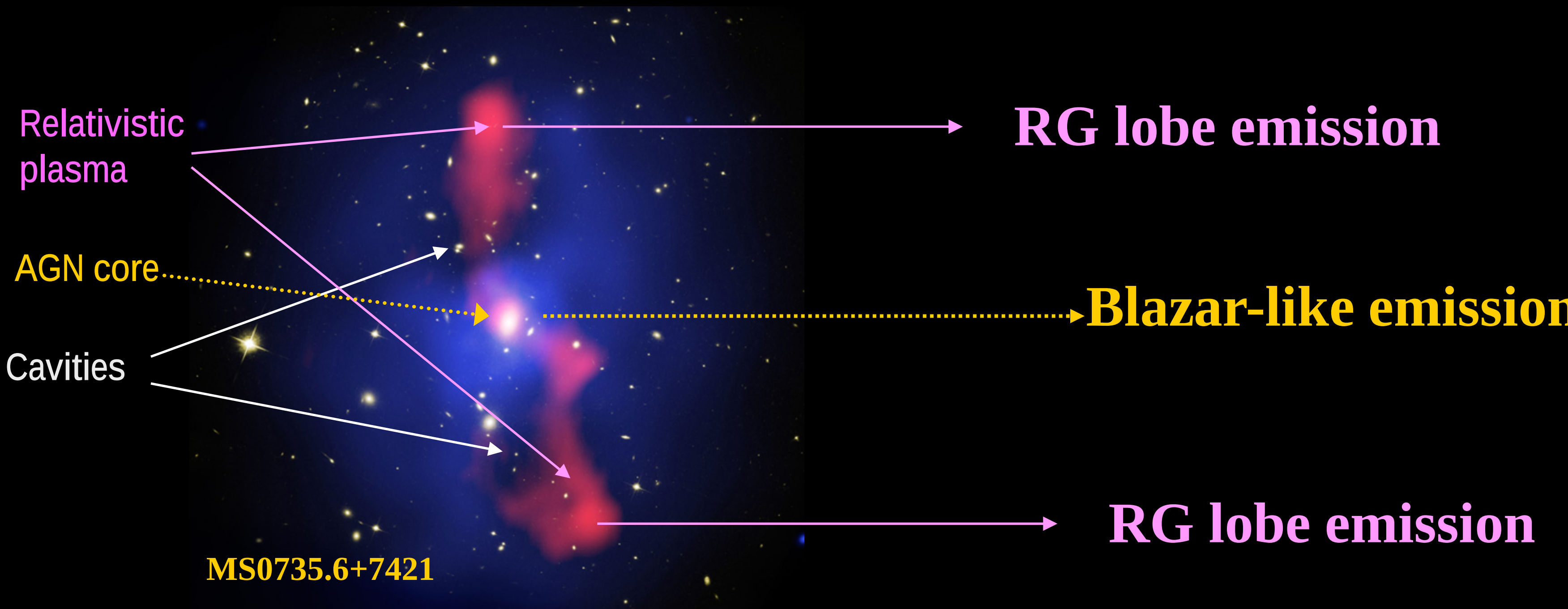

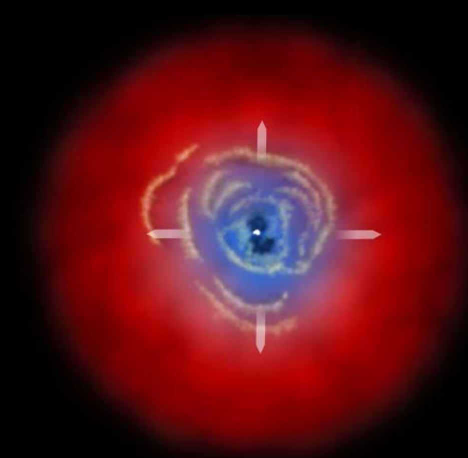

Cooling or not cooling ?

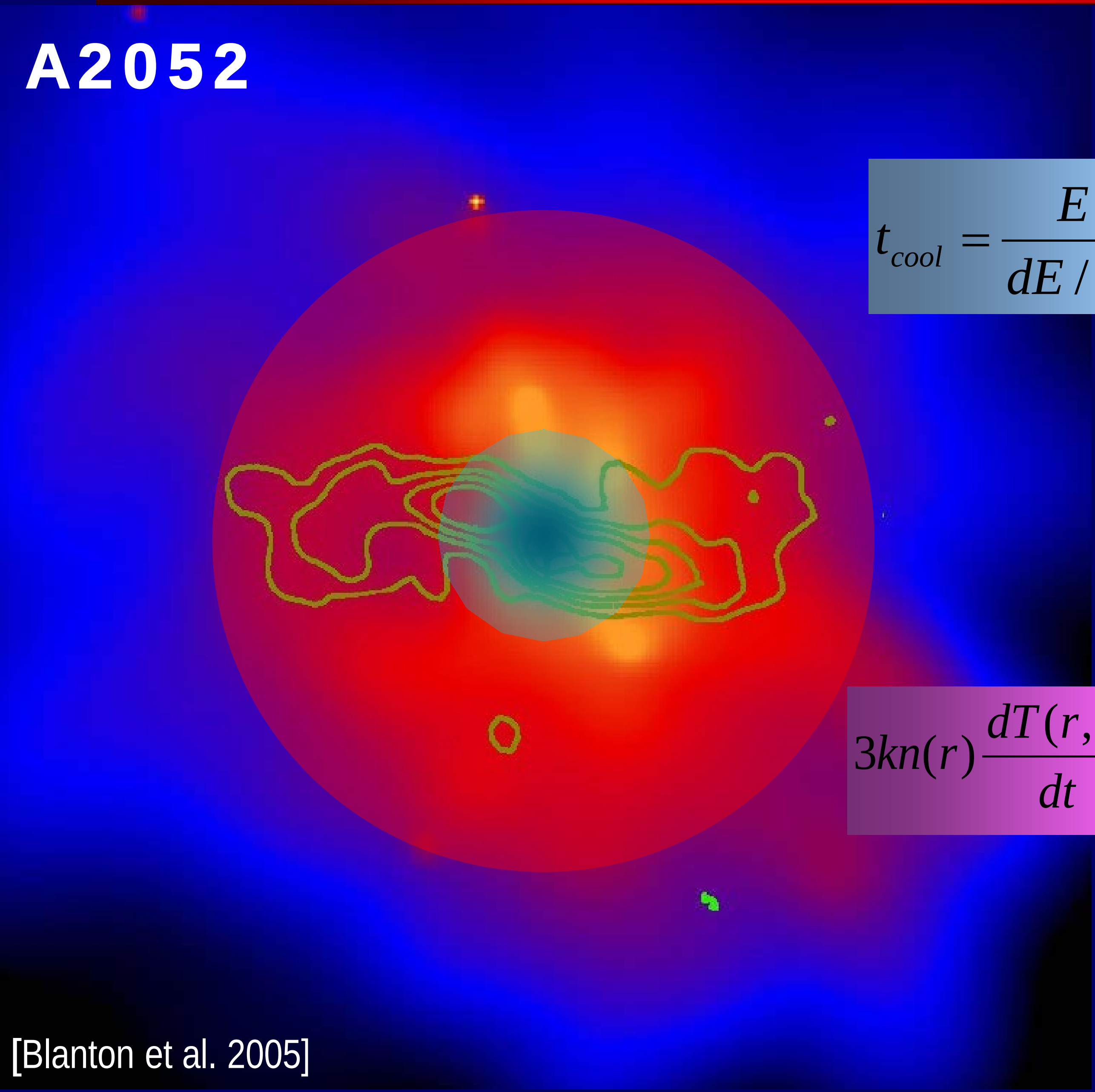

$$t_{cool} = \frac{E}{dE/dt} = \frac{E}{L} \approx \frac{nkT}{n^2\sqrt{kT}} = \frac{\sqrt{kT}}{n}$$

cooling

$$3kn(r)\frac{dT(r,t)}{dt} = \qquad - \left(\frac{dE}{dt}\right)_{cooling}$$

heating

Cluster cool cores

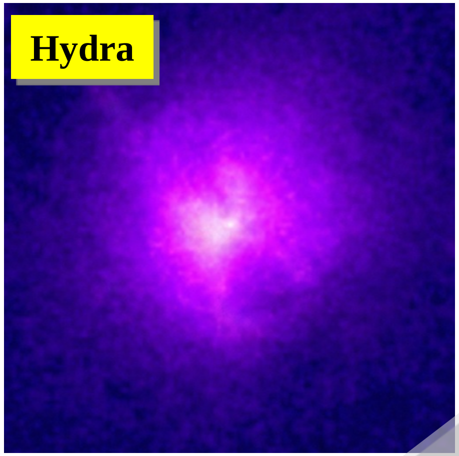

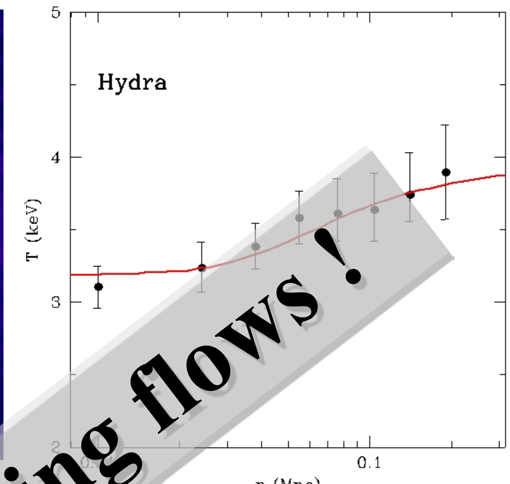

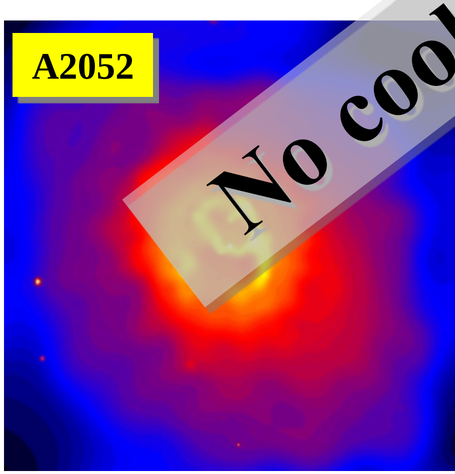

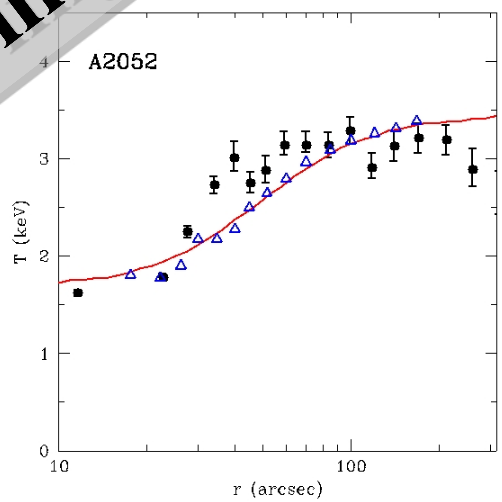

No cooling flows !

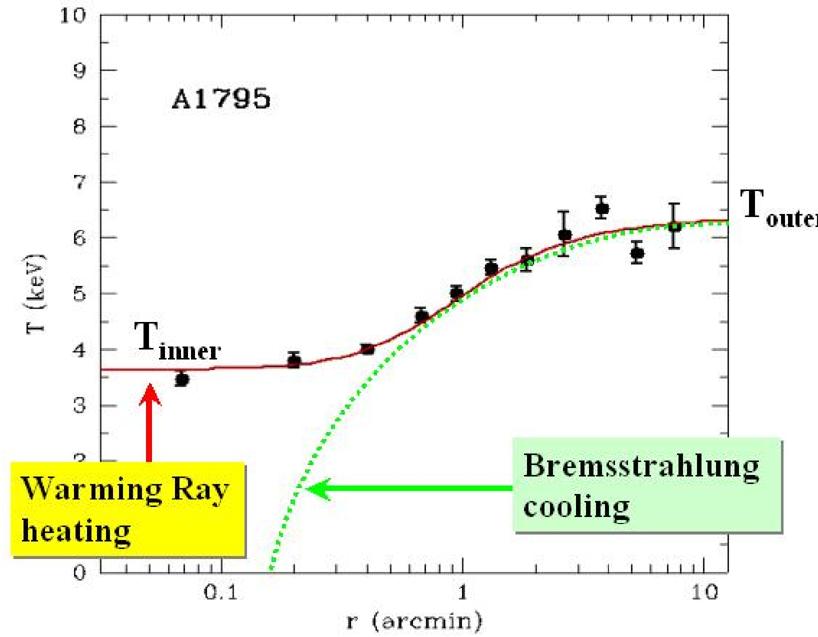

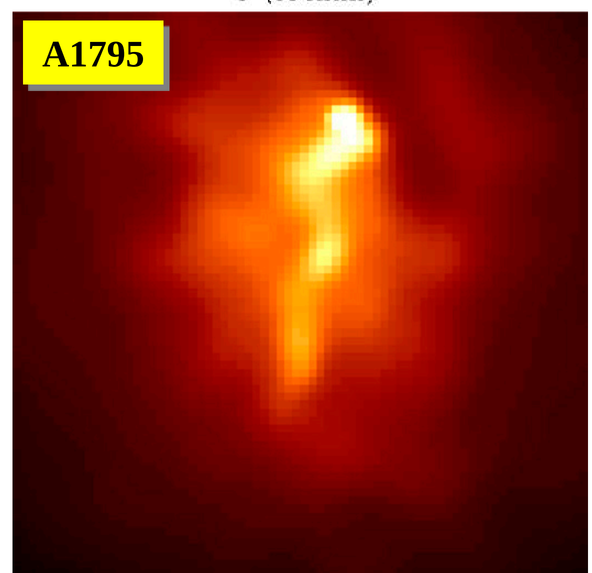

[S.C. Dar & DeRujula (2004)]

[S.C. (2005)]

[S.C. & Marchegiani (2008)]

Galaxy Clusters: crossroads of cosmic physics

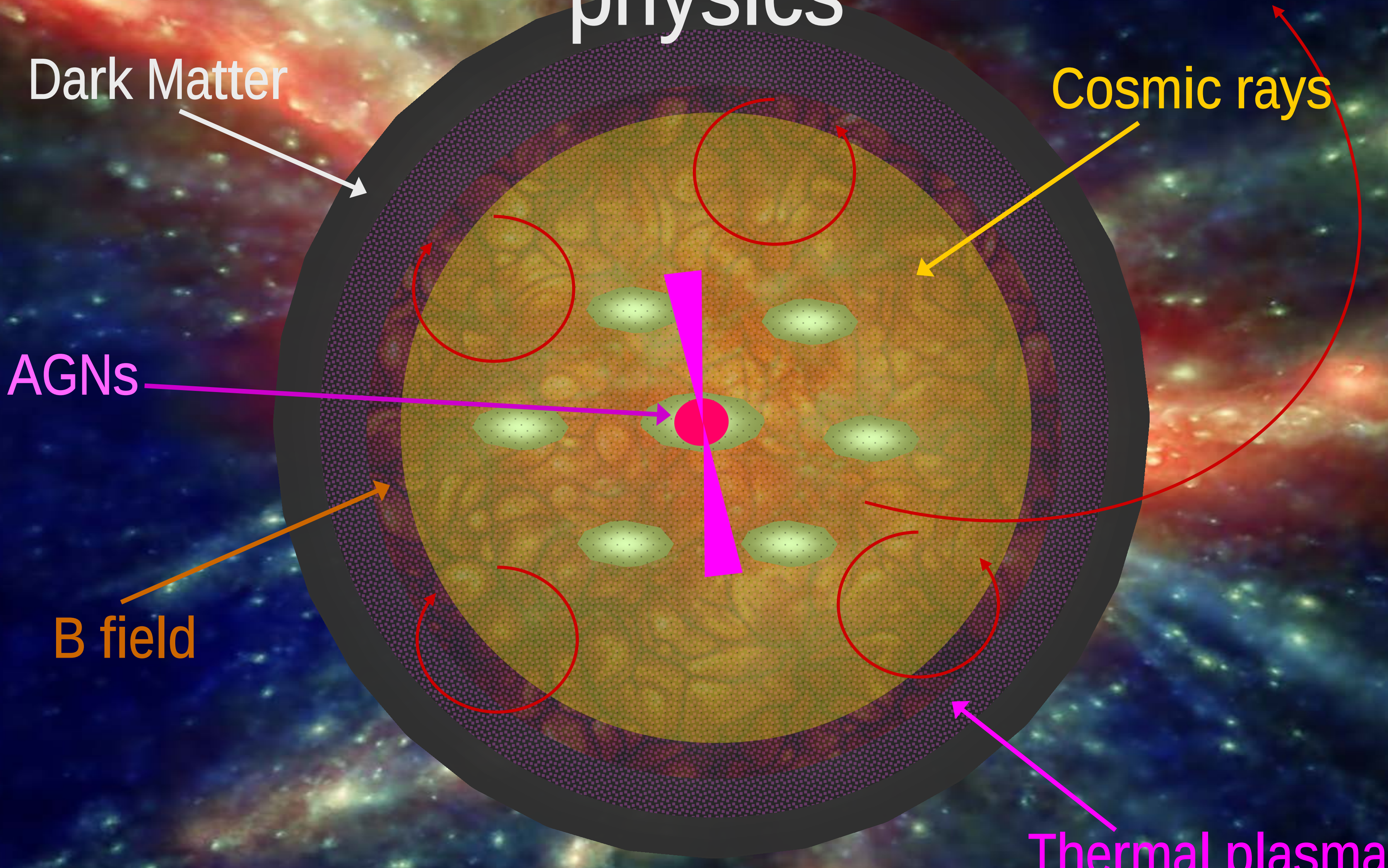

Cluster-RG interaction: Perseus core

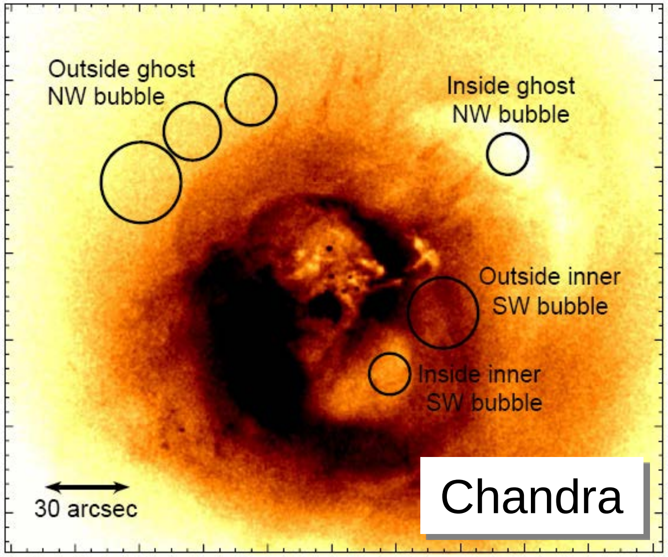

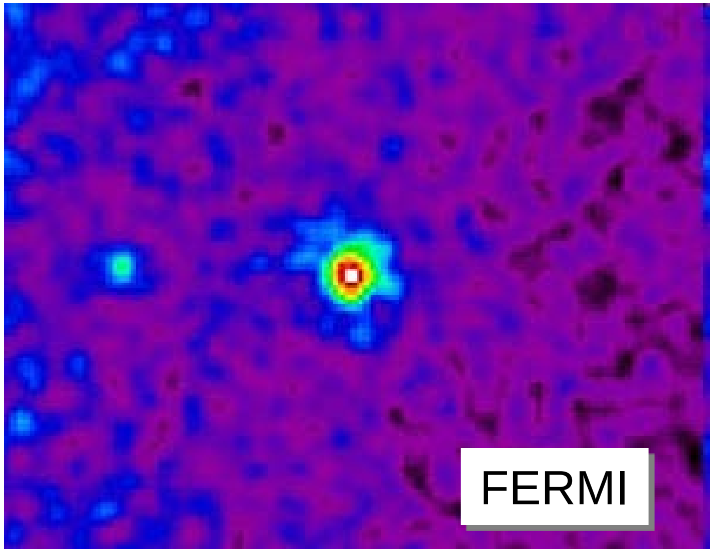

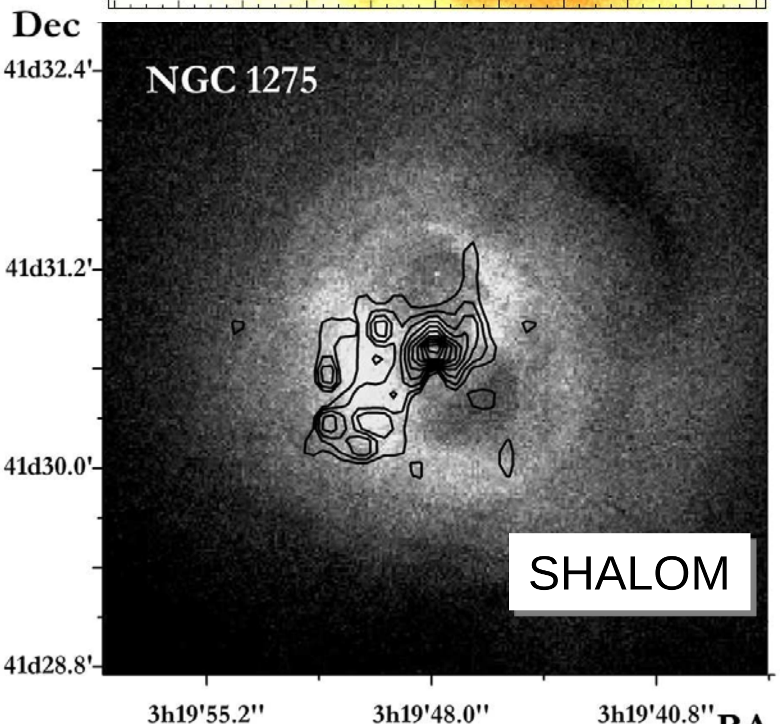

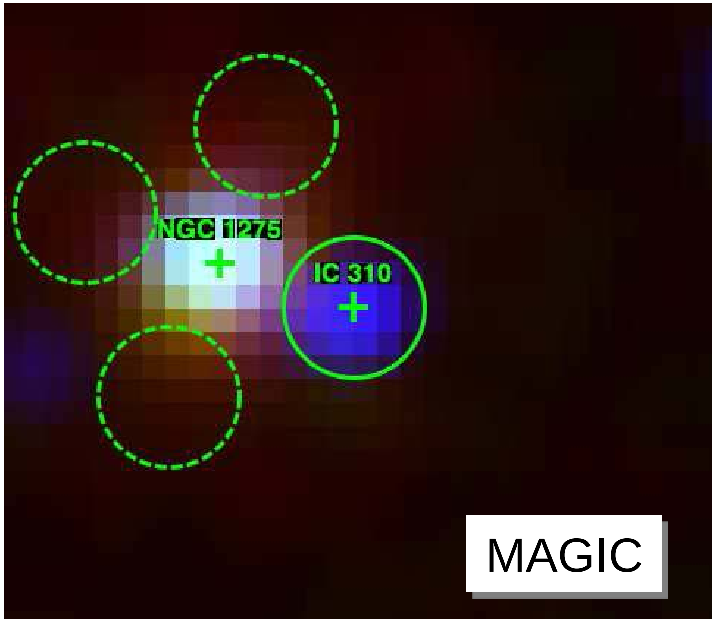

Perseus and NGC1275

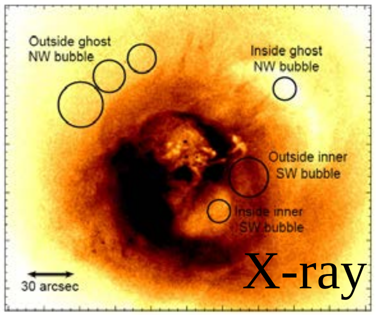

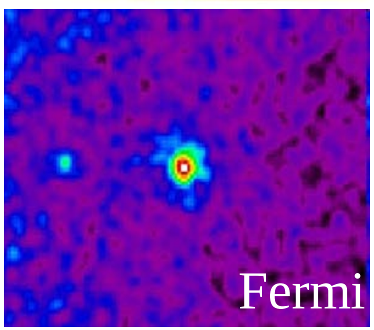

The SED is dominated by NGC1275 except for:

- Very low radio frequency: Perseus mini halo
- Soft X-rays: thermal gas bremsstrahlung

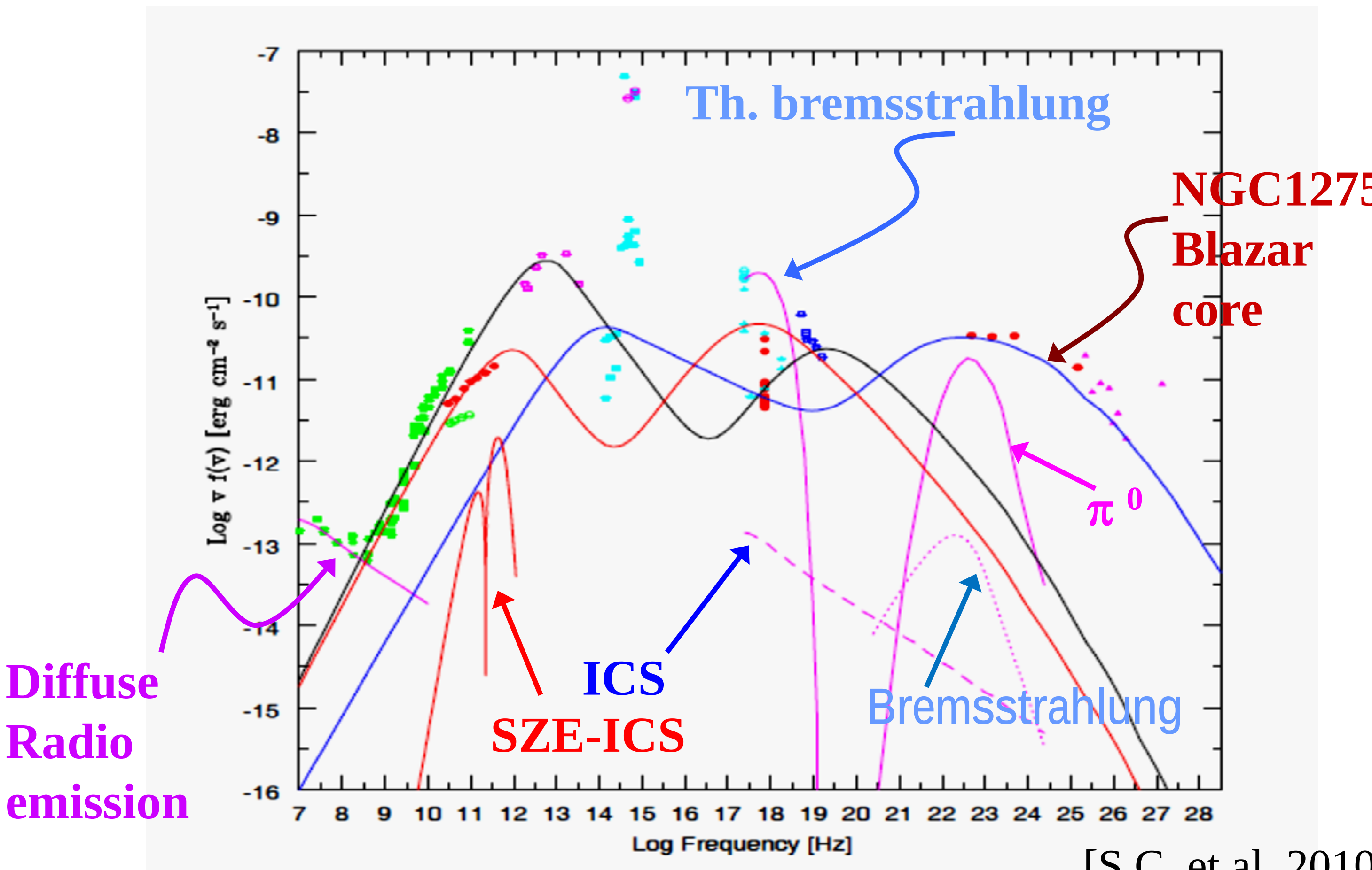

[S.C. et al. 2010]

Radio galaxies: jets and lobes

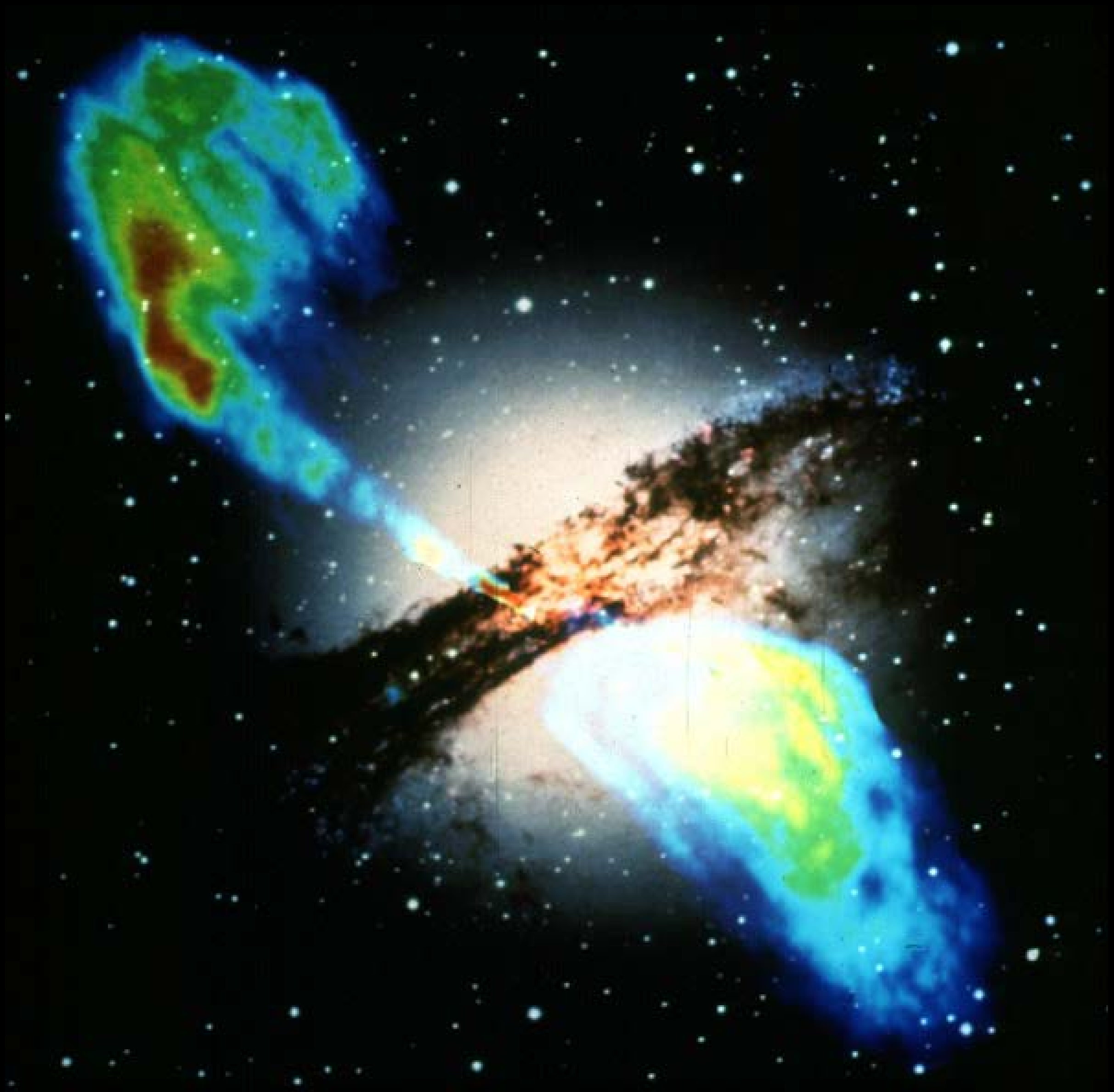

RGs: jet / lobe diffuse emission

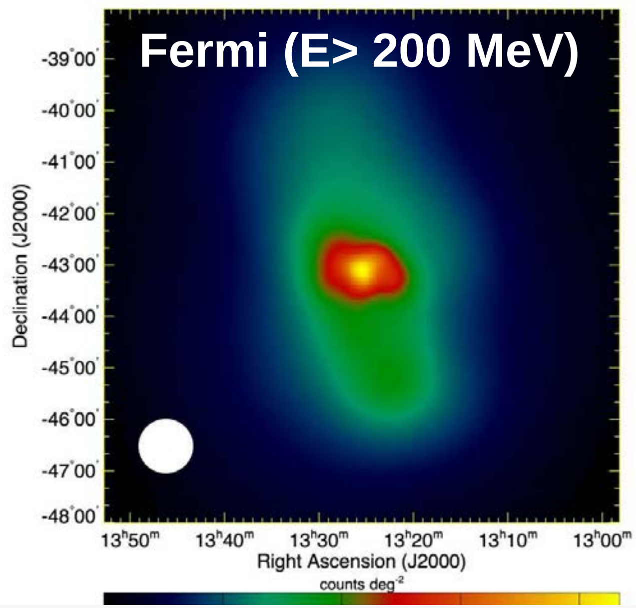

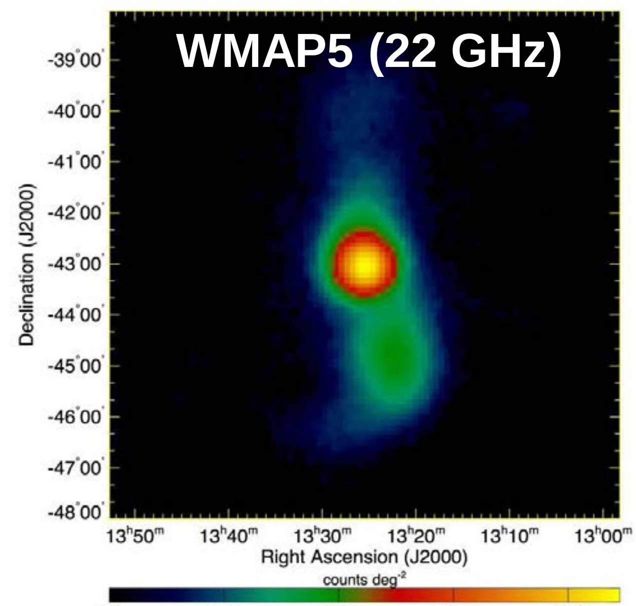

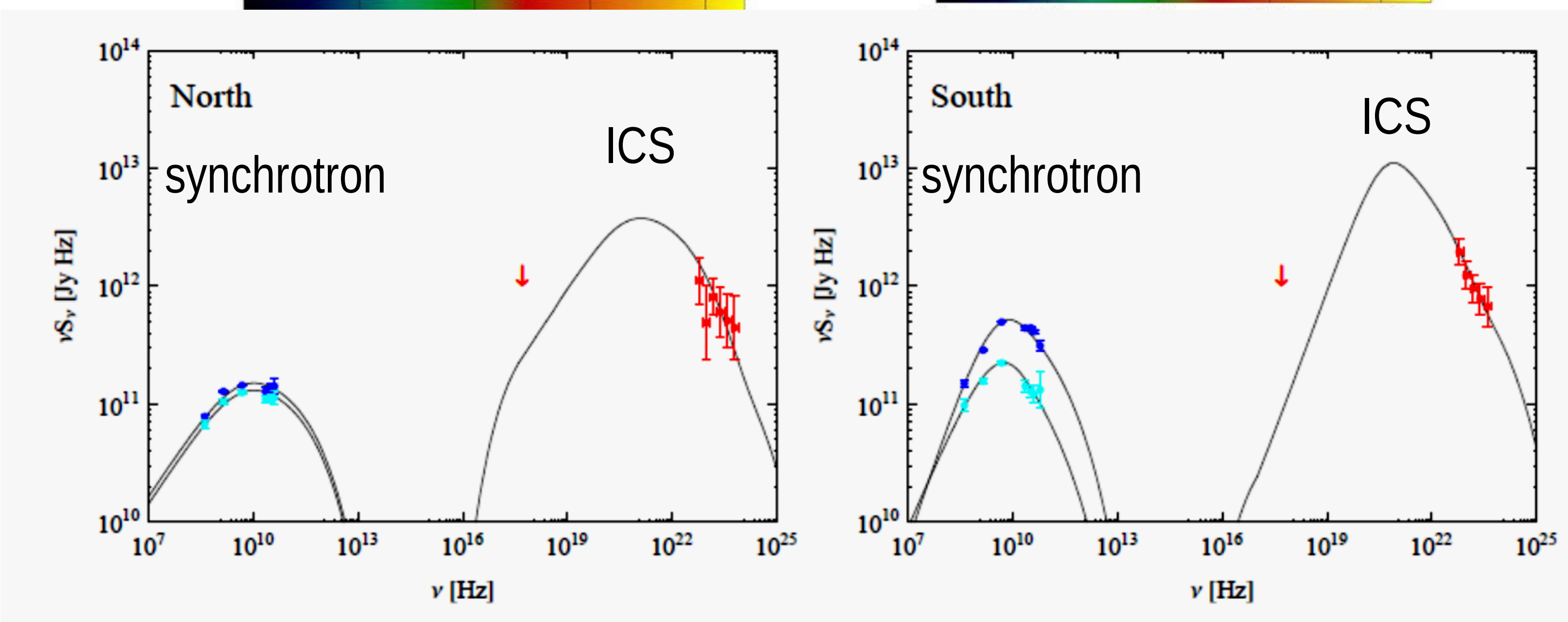

RGs: jet / lobe diffuse emission

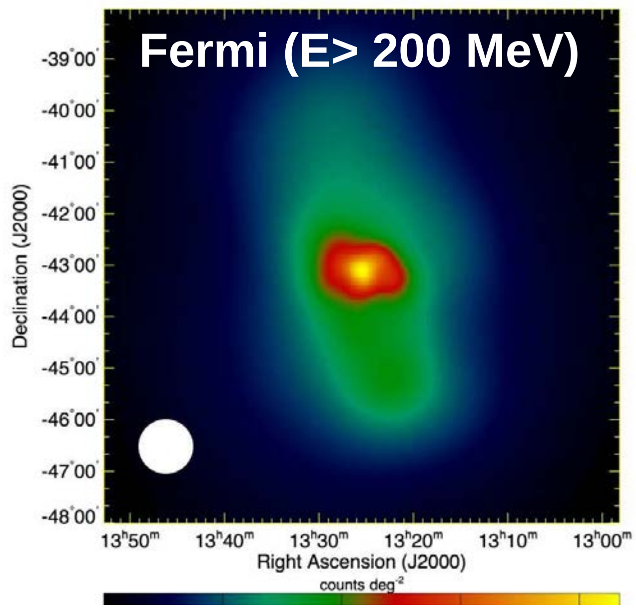

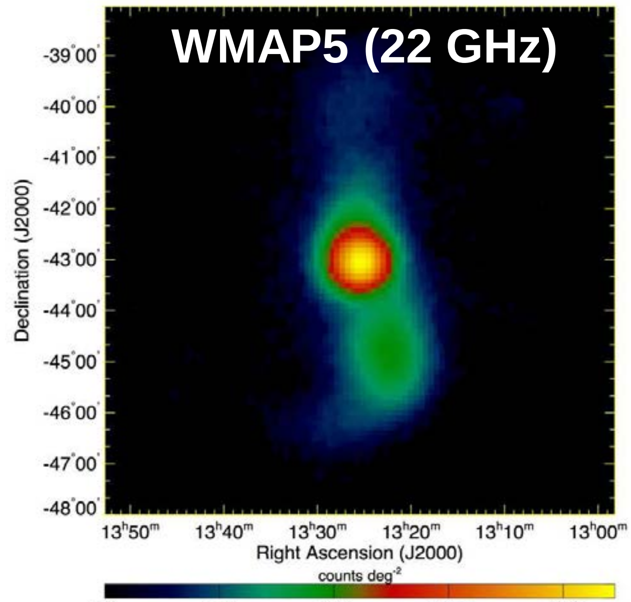

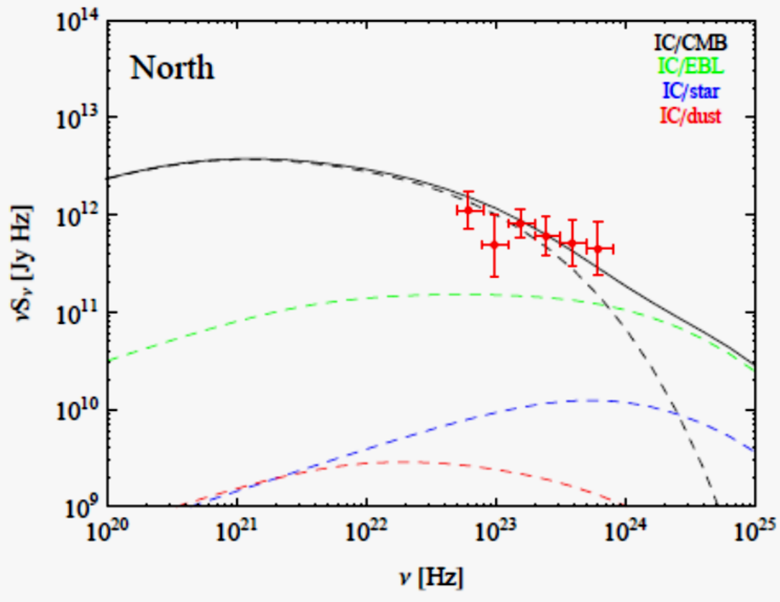

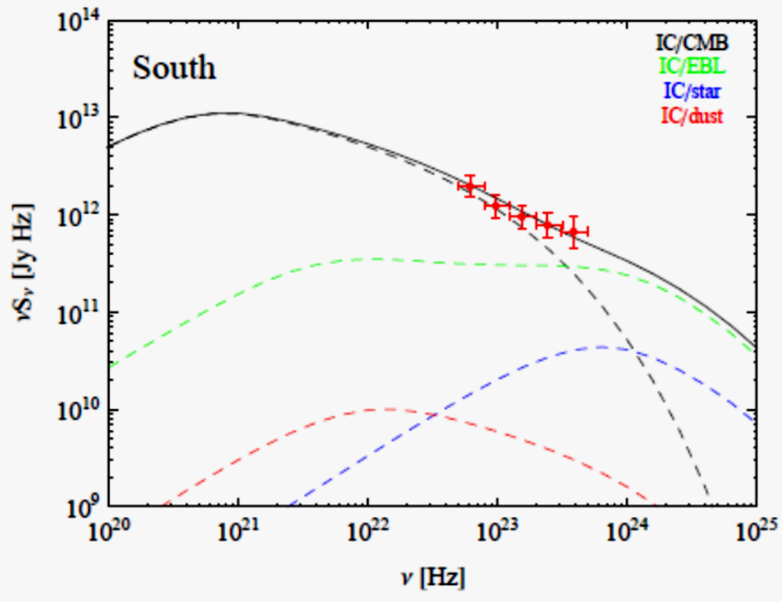

Radiogalaxy jets: emission

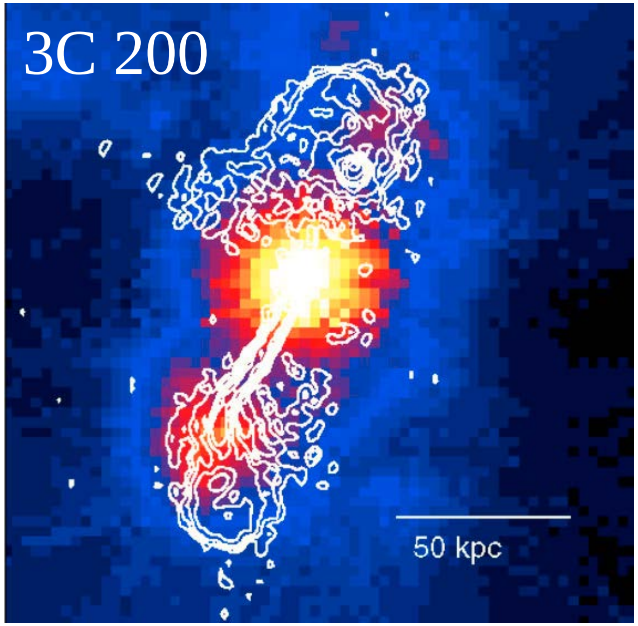

Chandra (color)+5GHz (contours)

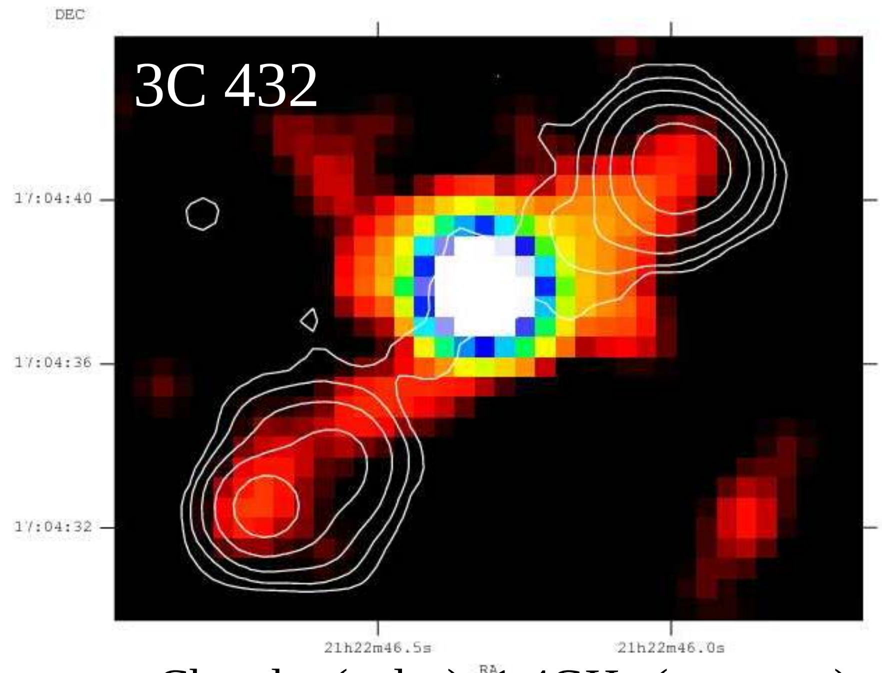

Chandra (color)+1.4GHz (contours)

$$F_{radio} \approx \nu^{-\alpha} B^{2(\alpha+1)} \qquad F_{X-ray} \approx E^{-\alpha}$$

$$\alpha = (p-1)/2$$

The co-spatial location and the similarity in the X-ray and radio spectra indicate a common parent population → $N_e \sim E^{-p}$ for the electrons responsible for the jet/lobe emission

CenA: more properties

Cen-A at multi-frequency

Xrays
Radio
Optical

High-ν polarization information crucial to unveil magnetic field structure and the sites of particle acceleration

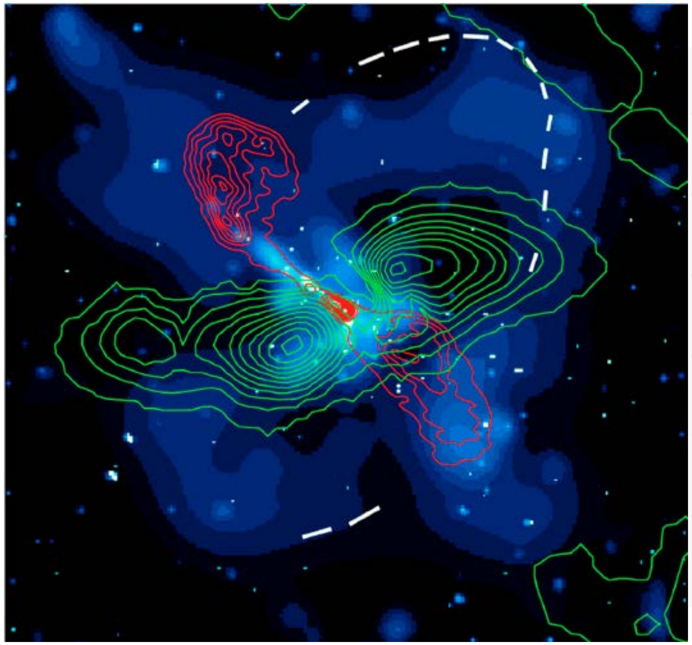

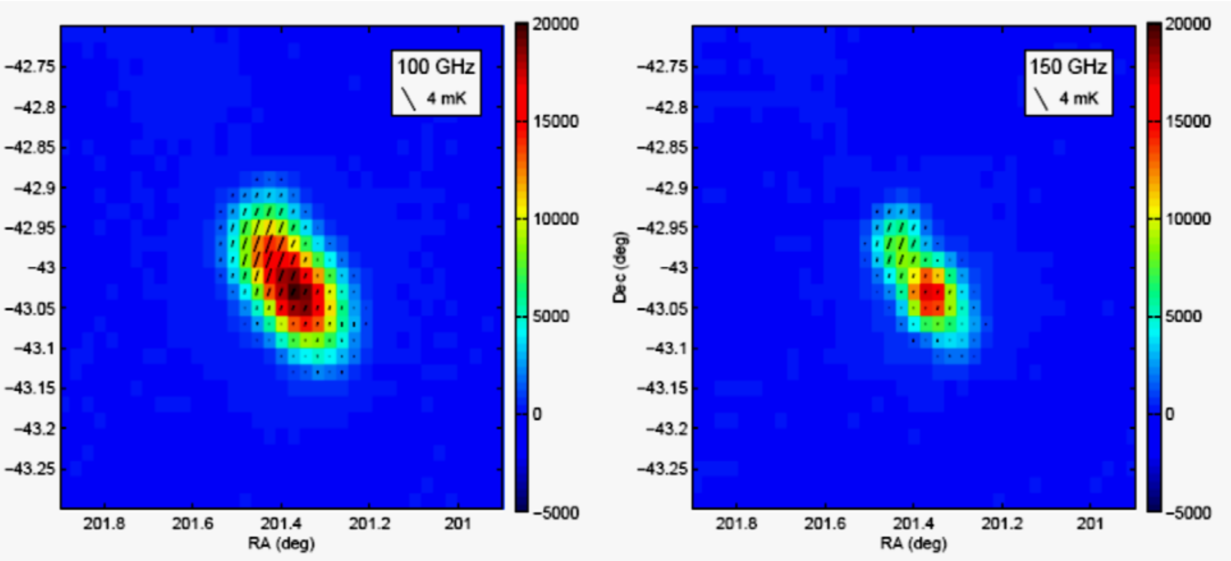

Very high polarized radio lobes

CGCG 049-033: well collimated radio jet, largest detected jet, very strongly polarized (P ~20 to 50% at 8 GHz) [Bagchi et al. 2009]

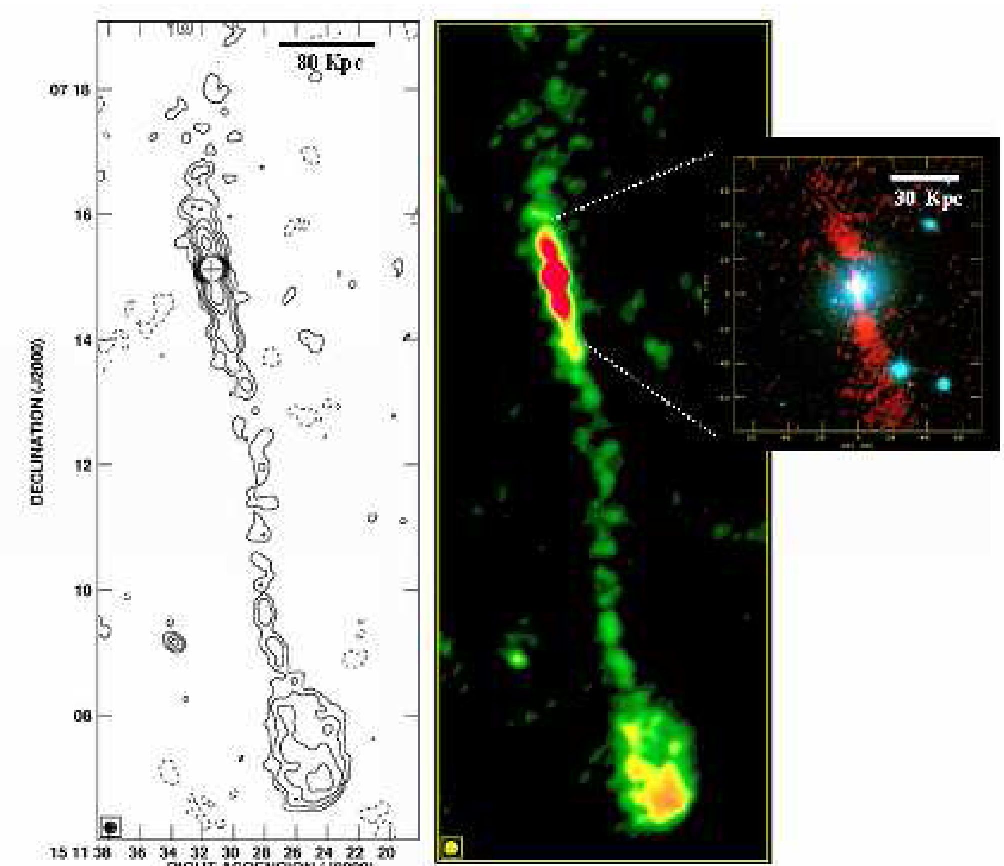

GMRT and VLA maps of CGCG 049-033 with contours at: -0.18, 0.18, 0.36, 0.72, 1.44, 3 and 6 mJy/beam

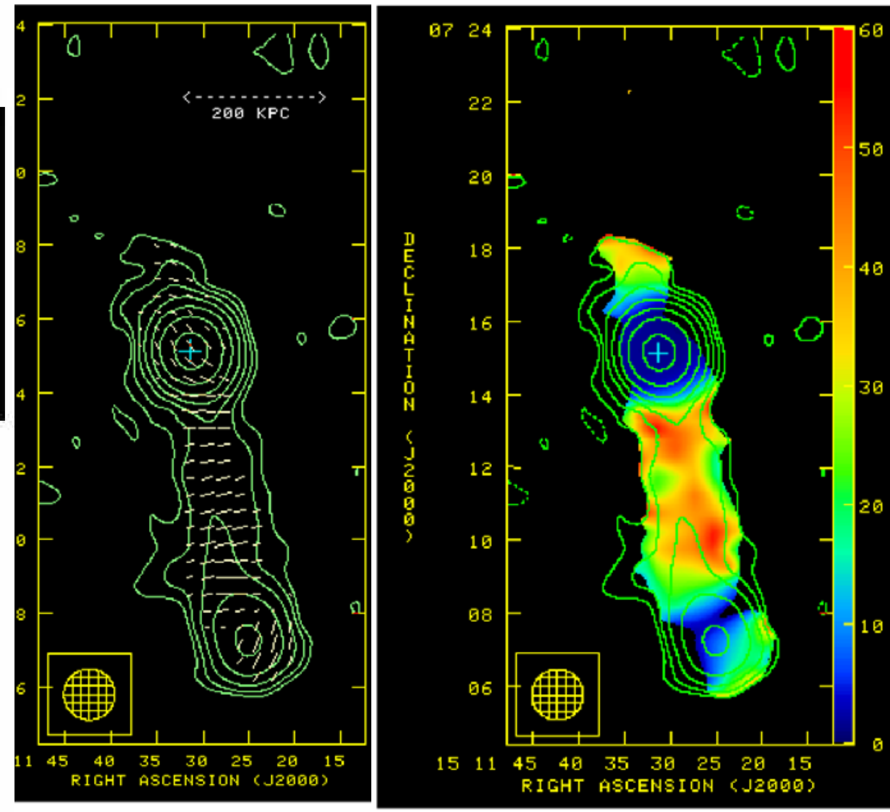

Effelsberg 8.35 GHz total power contour map: -0.75, 0.75, 1.5, 3, 6, 12, 24 and 48 mJy/beam

RGs: 3D tomography of jets

Farady Rotation polarization

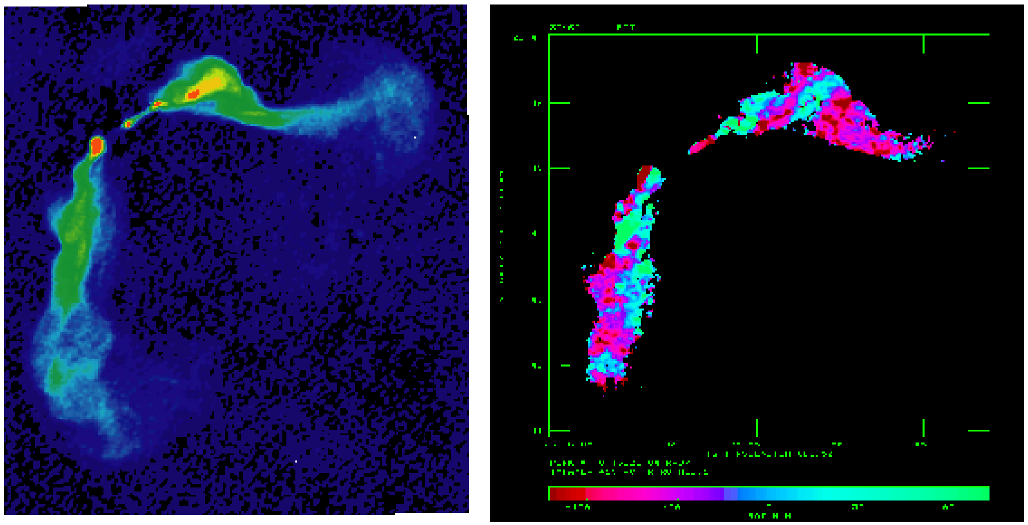

3C465, an AGN; Synchrotron Emission; Faraday Rotation of underlying polarization.
Eilek and Owen, 2000.

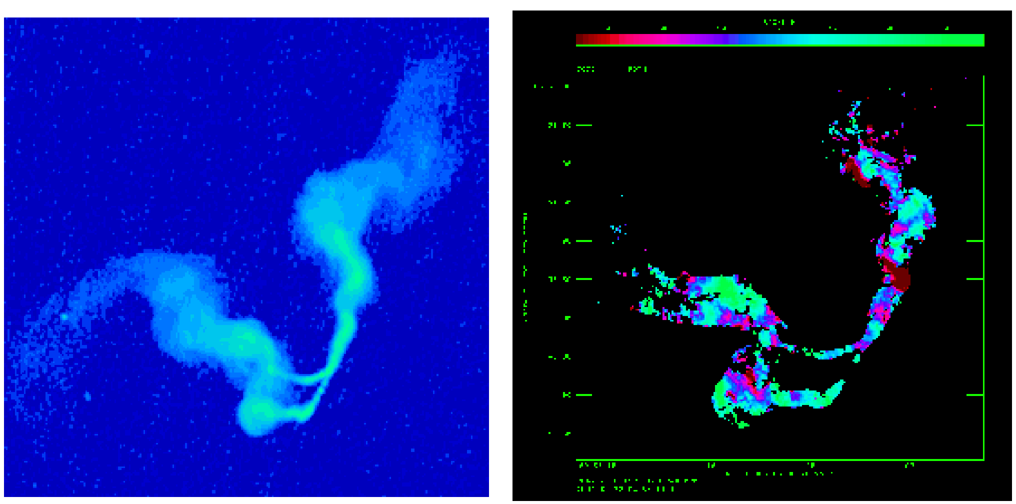

3C75, an AGN; Synchrotron Emission; Faraday Rotation of underlying polarization.
Eilek and Owen, 2000.

Fornax A radio galaxy lobes

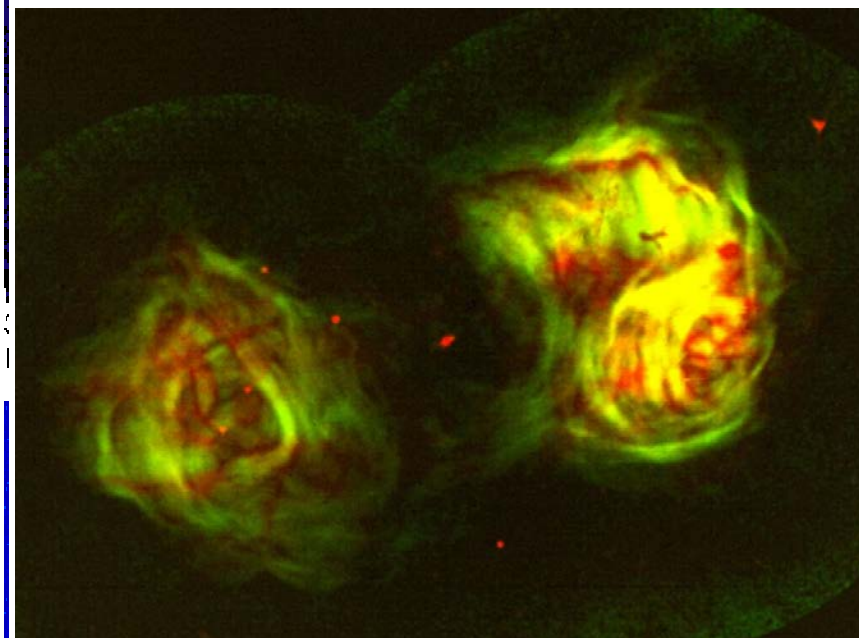

Radio synchrotron polarization

RG jets / lobes: simulations

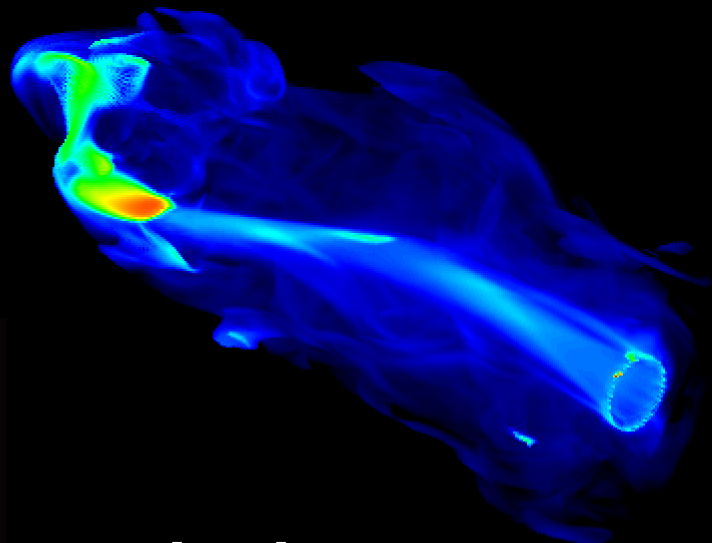

Synchrotron brightness at 5.4 GHz

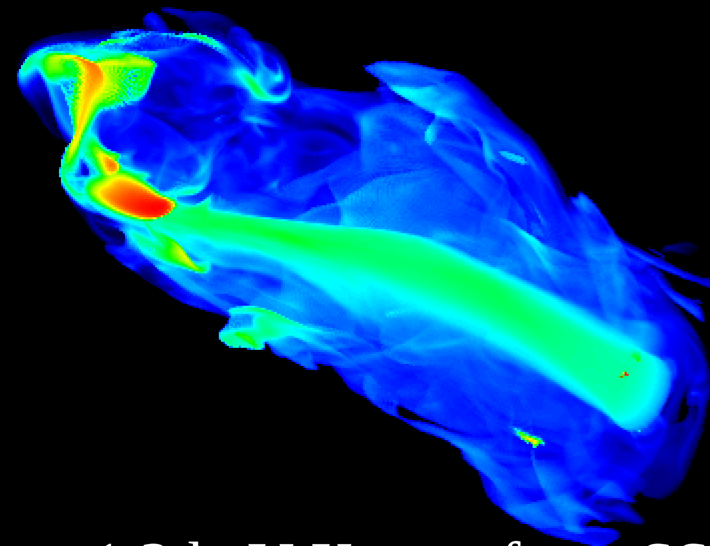

1.2 keV X-rays from SSC

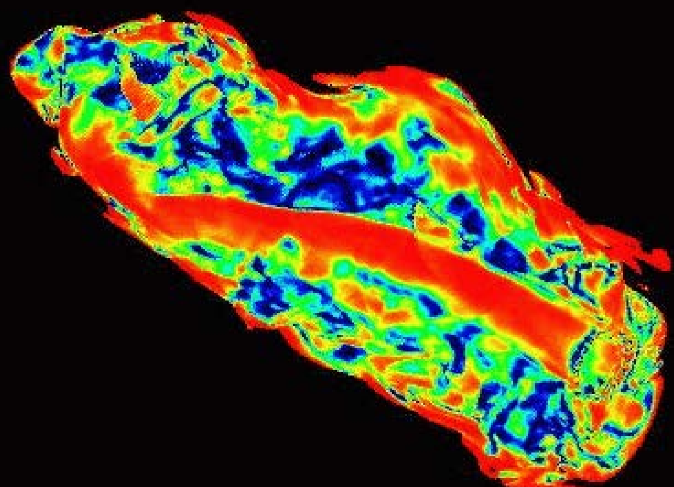

Fractional polarization

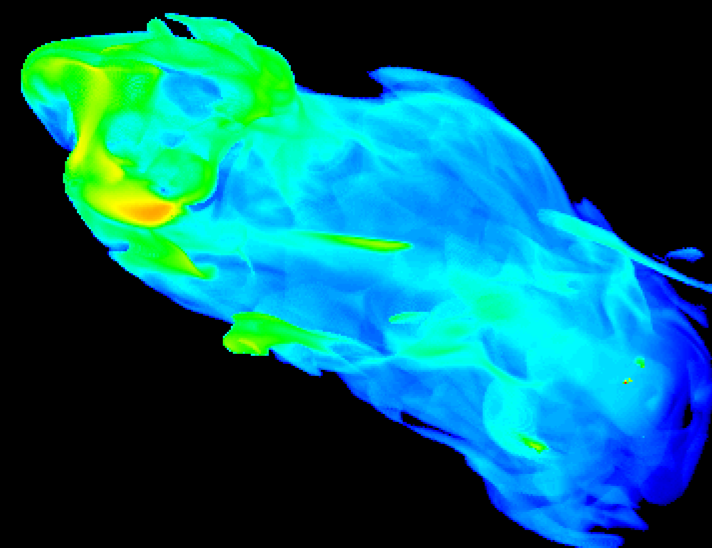

1.2 keV X-rays from IC-on-CMB

RGs: lobes vs core emission

Extended Lobe emission decreases with frequency:

→ steep spectrum (diffuse emission)

Core emission remains visible at high frequency:

→ flat spectrum (Blazar like)

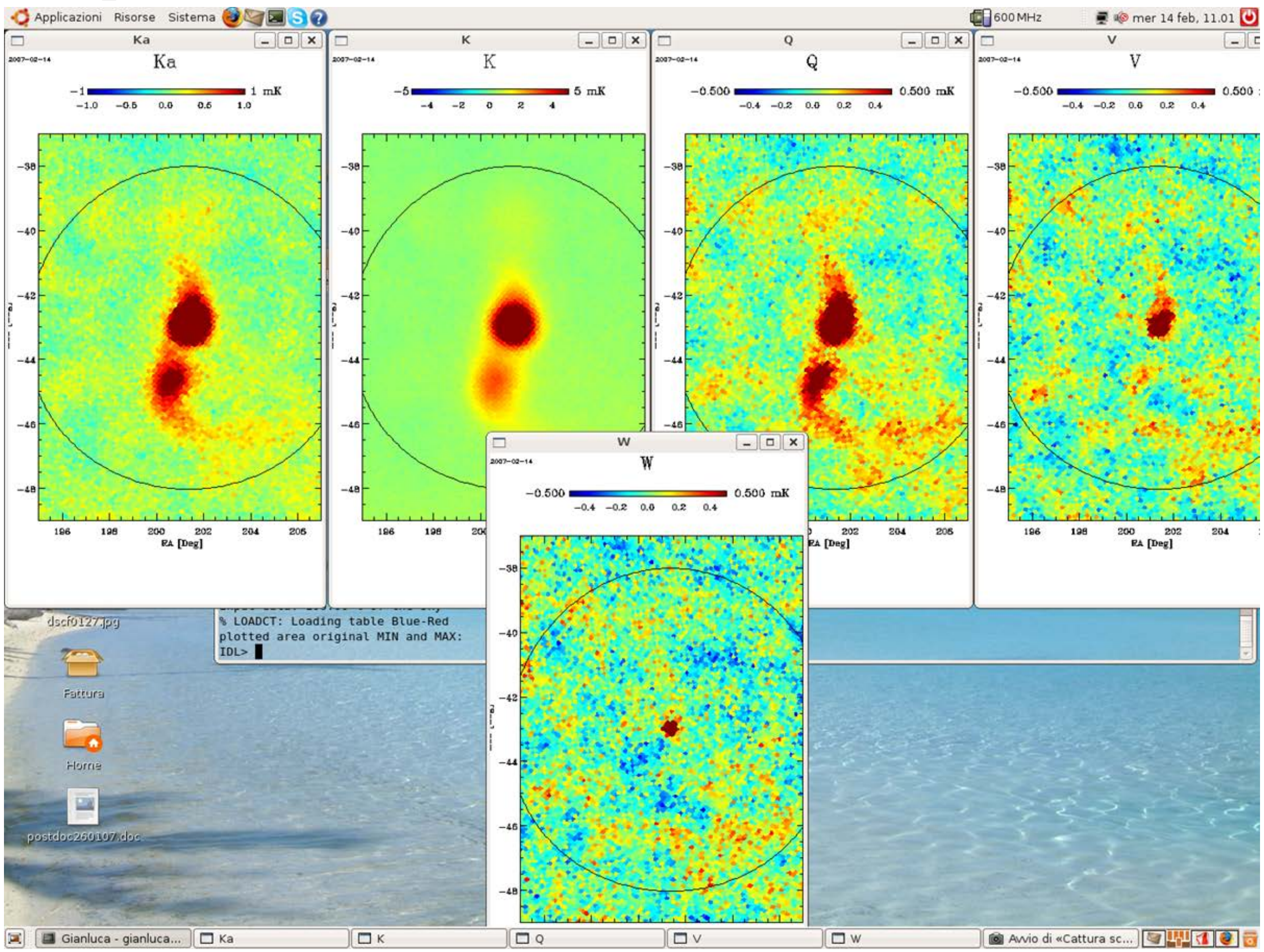

RG vs Blazar SEDs

Pictor A

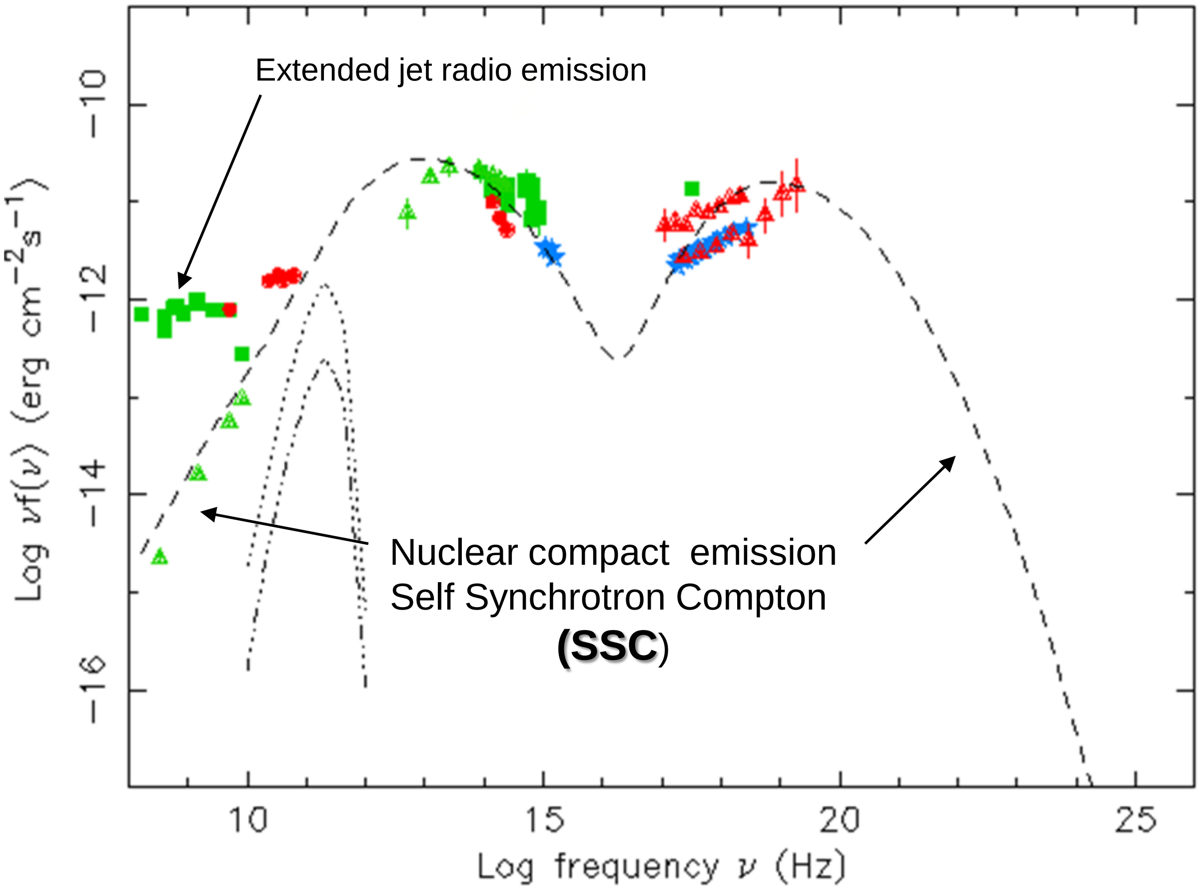

RGs vs Blazar SEDs

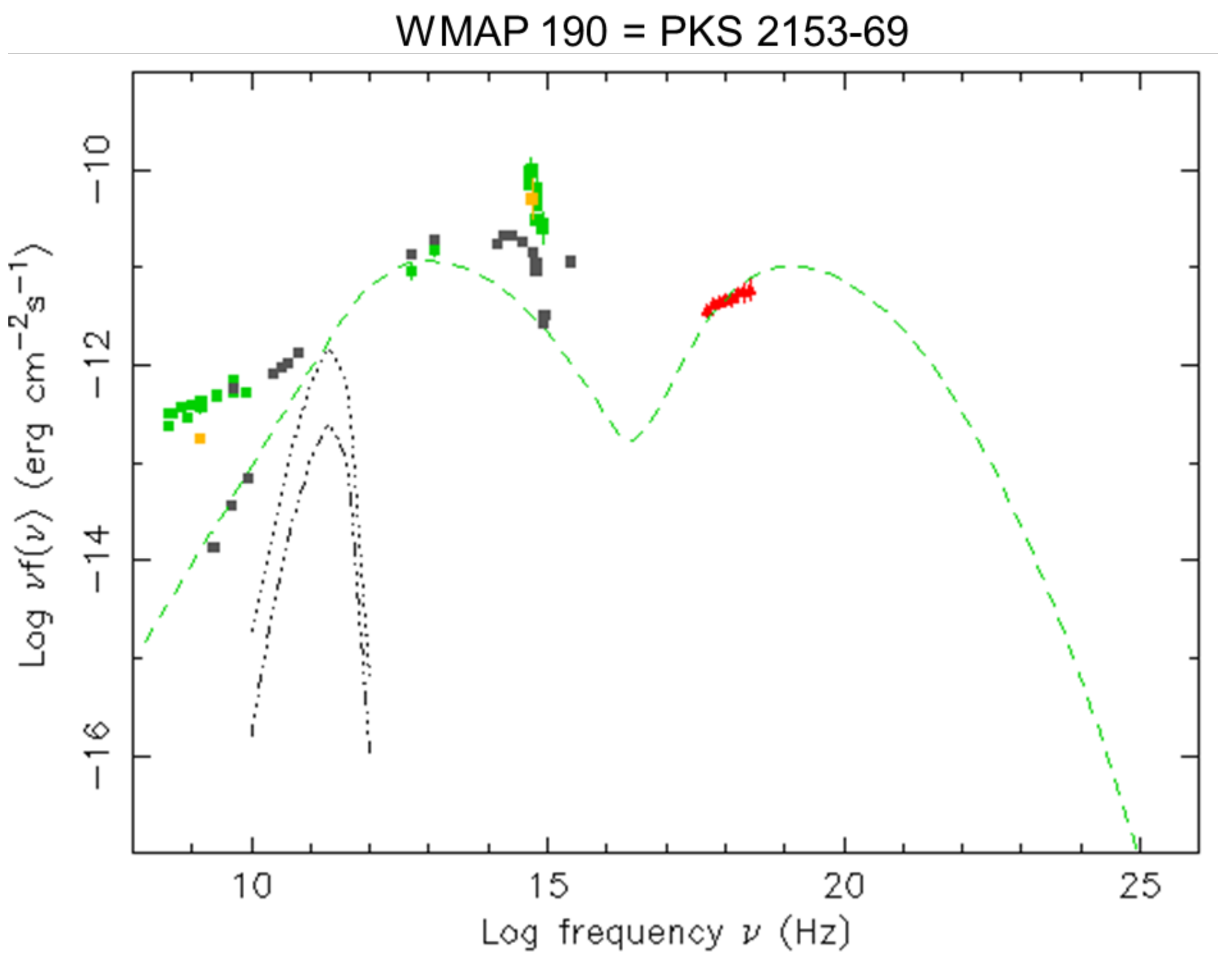

RG vs Blazar SEDs

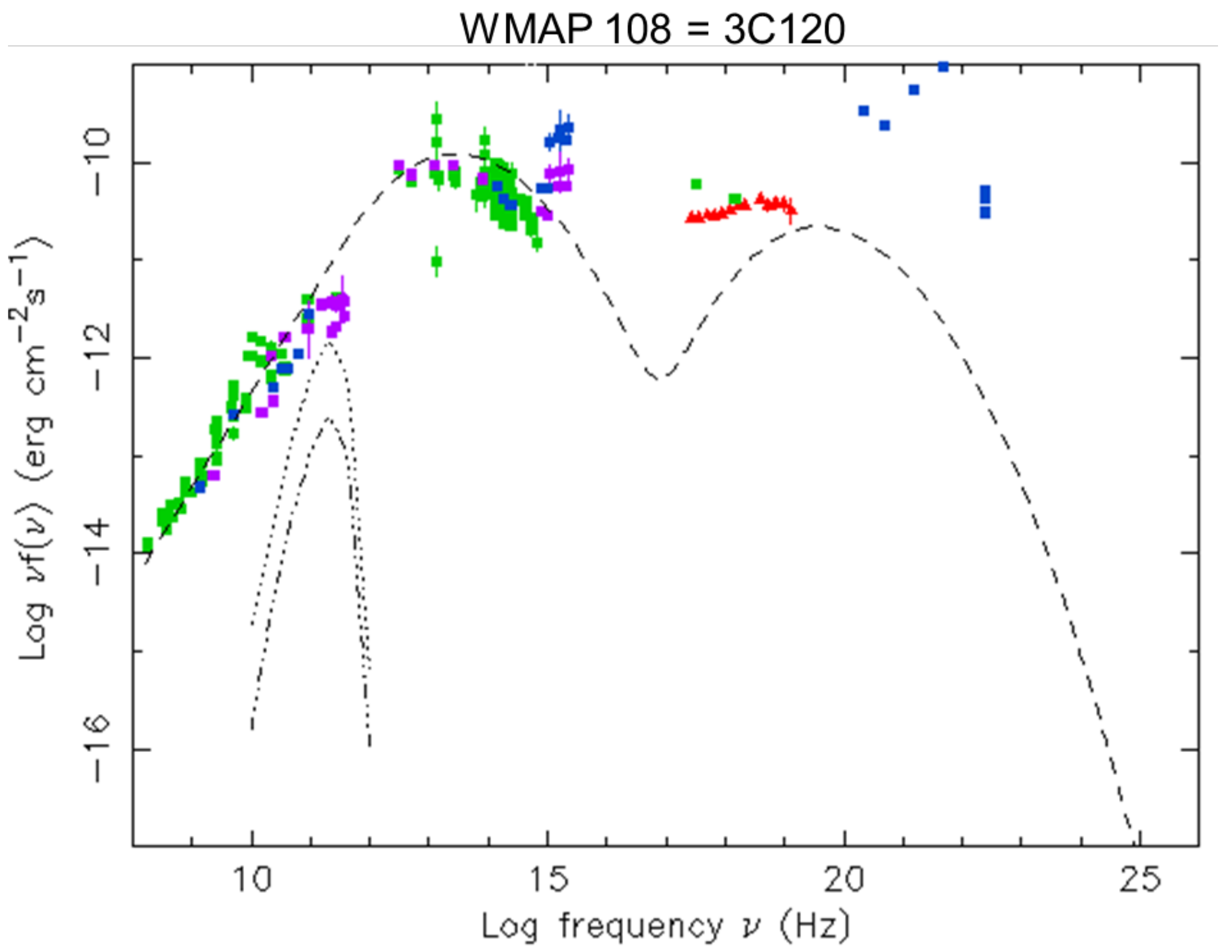

RG vs Blazar SEDs

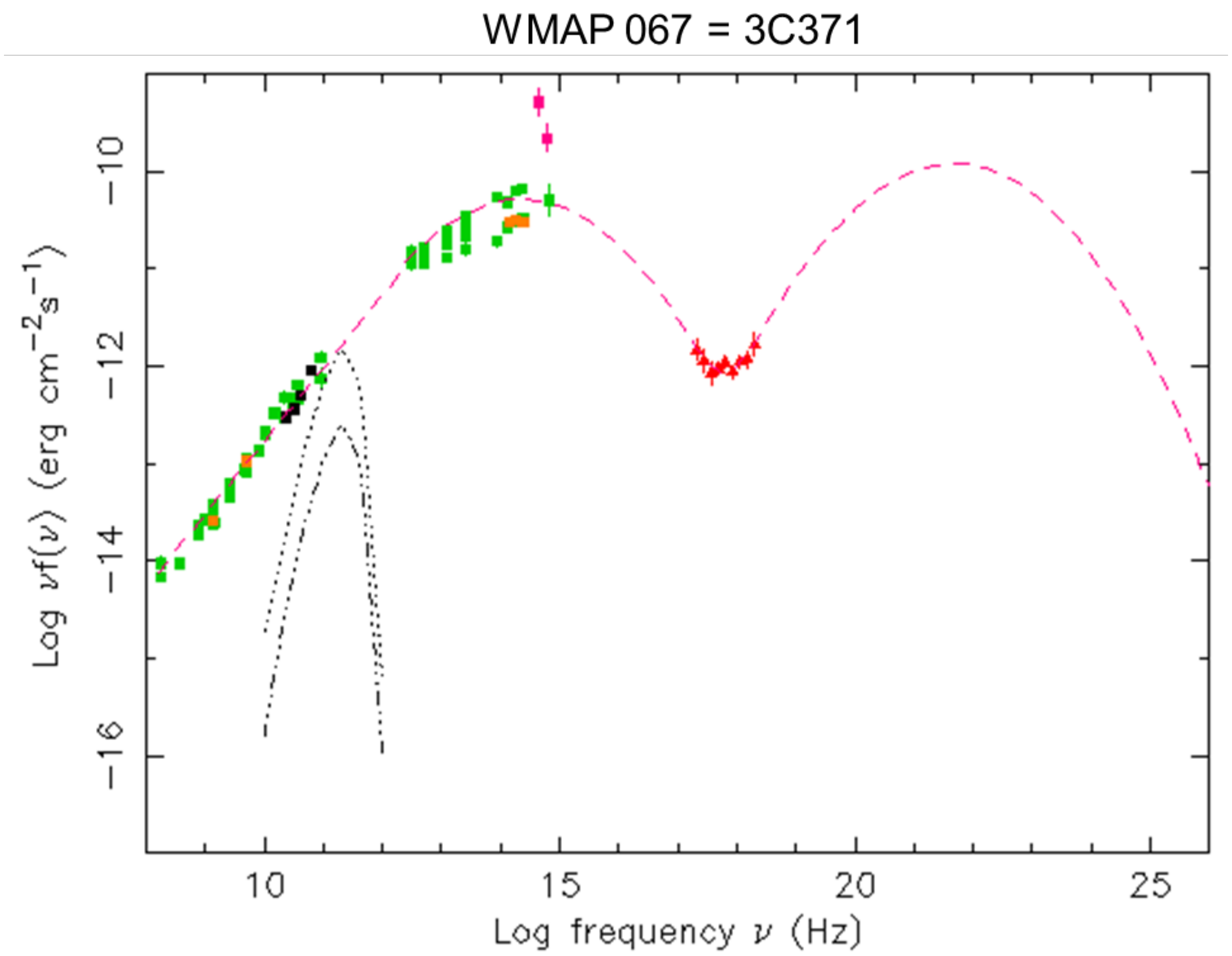

RG vs Blazar SEDs

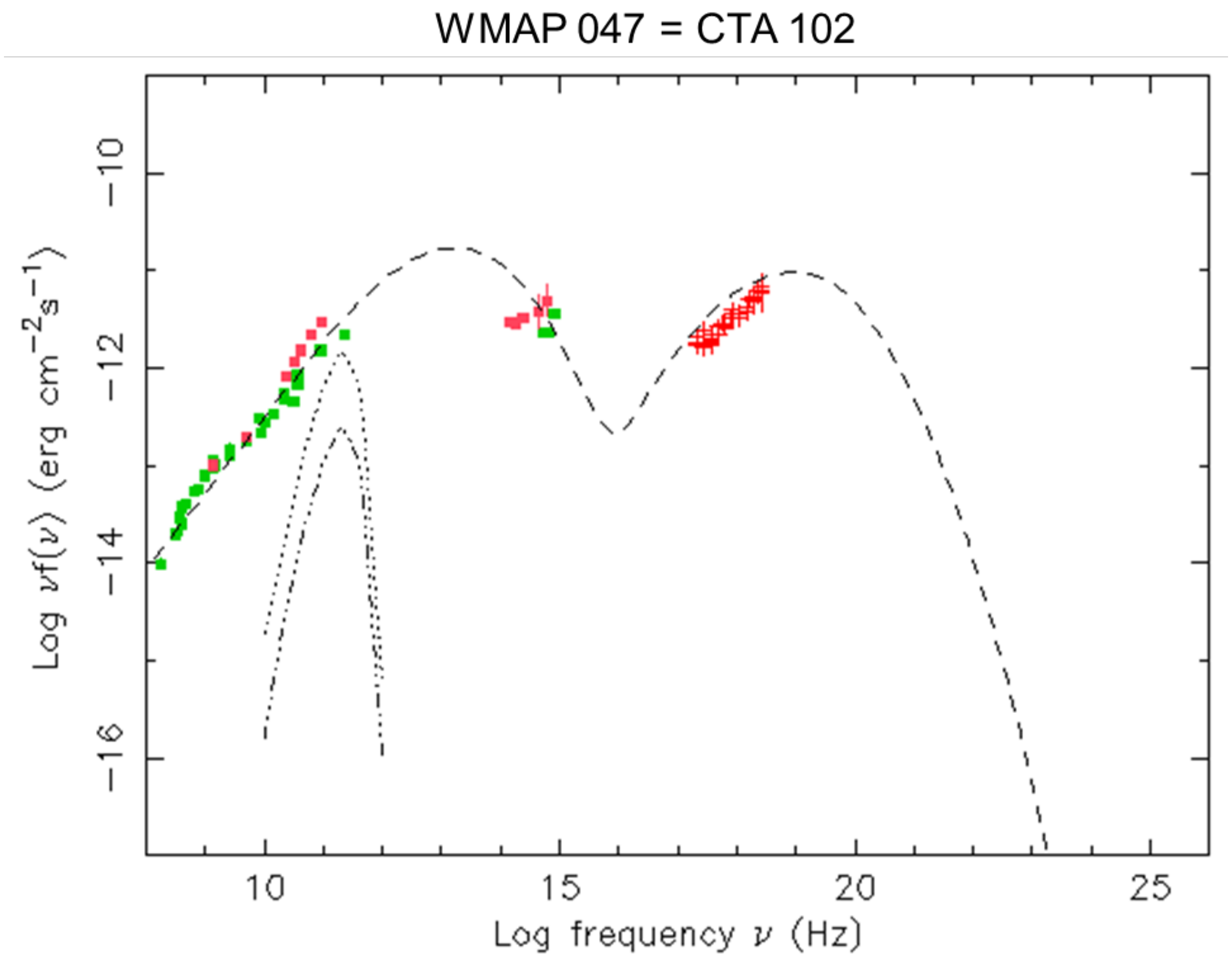

The AGN Zoo

DUAL energy band favours:

- **LSP** objects with large Compton dominance
  (flat spectra in DUAL, steep spectra in Fermi)
- **(U) HSP** with high flux (no Compton dominance)
  (steep spectra in DUAL, inverted spectra in Fermi)
- **Radiogalaxies** and **starbursts** in high activity states (nearby, high-L, flat spectra)

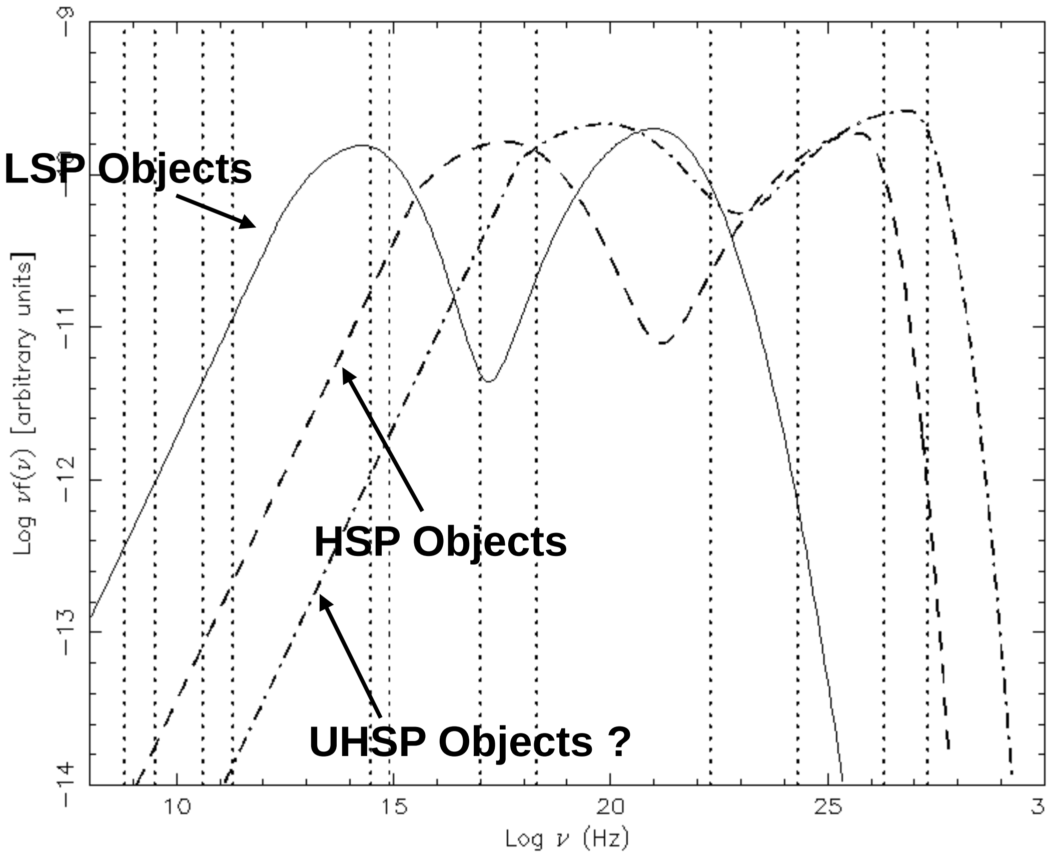

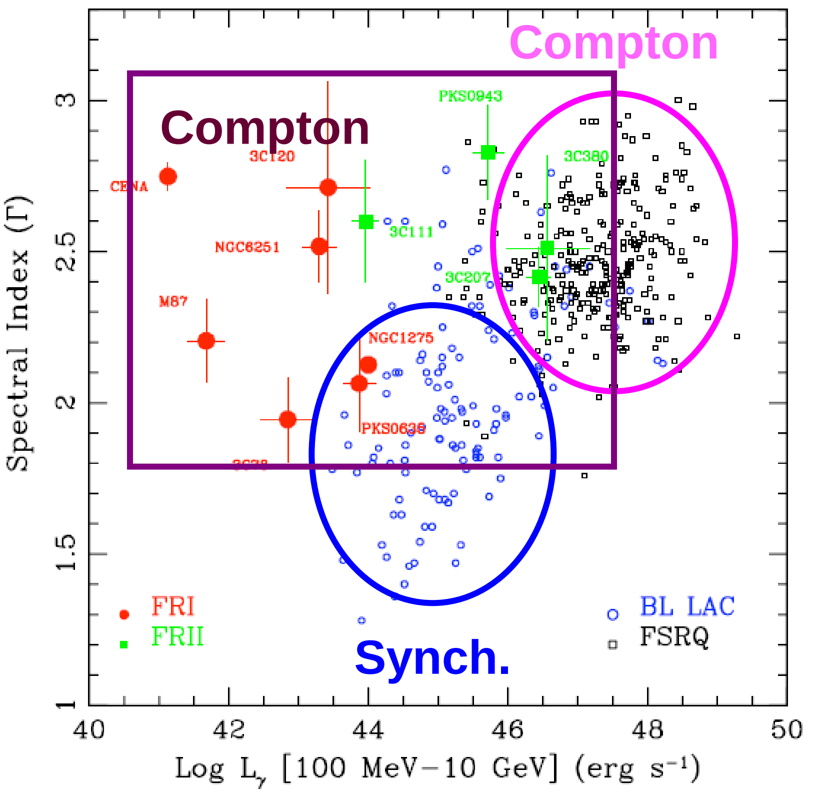

[Abdo et al. 2010]

RGs & Starbursts

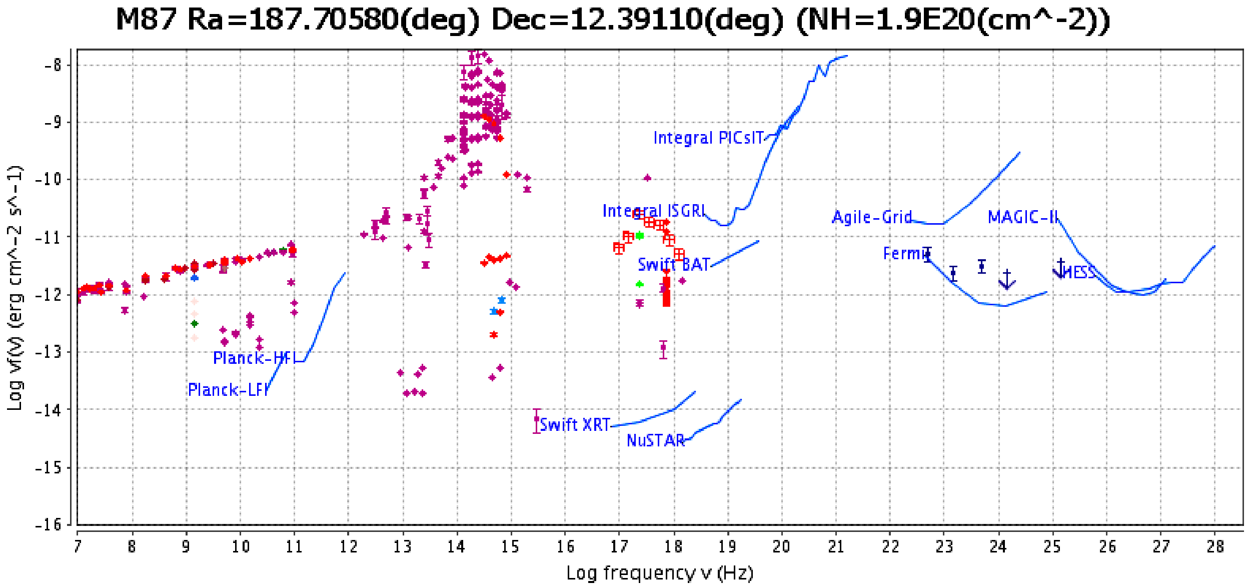

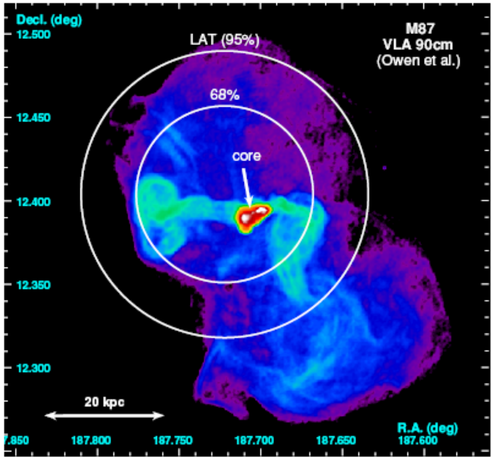

[Abdo et al. 2009 ApJ 707 55]

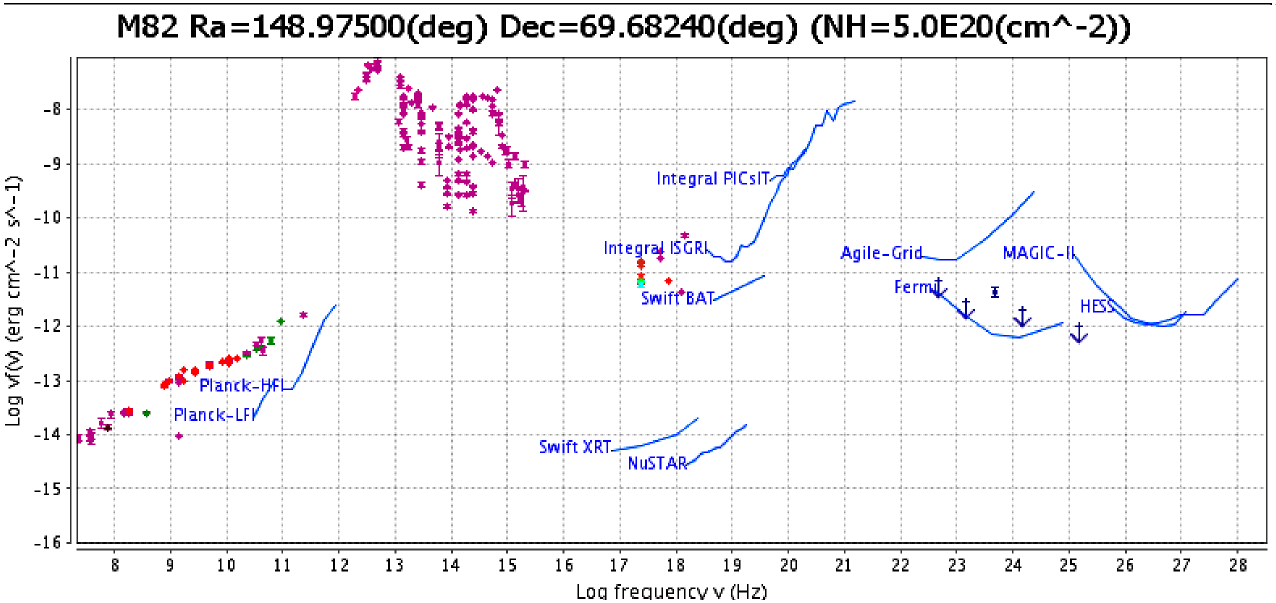

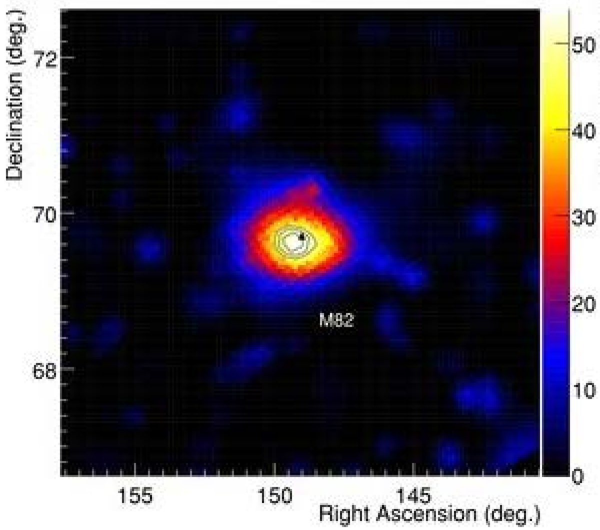

[Abdo et al. 709 (2010) L152]

Galaxy halos and outflows

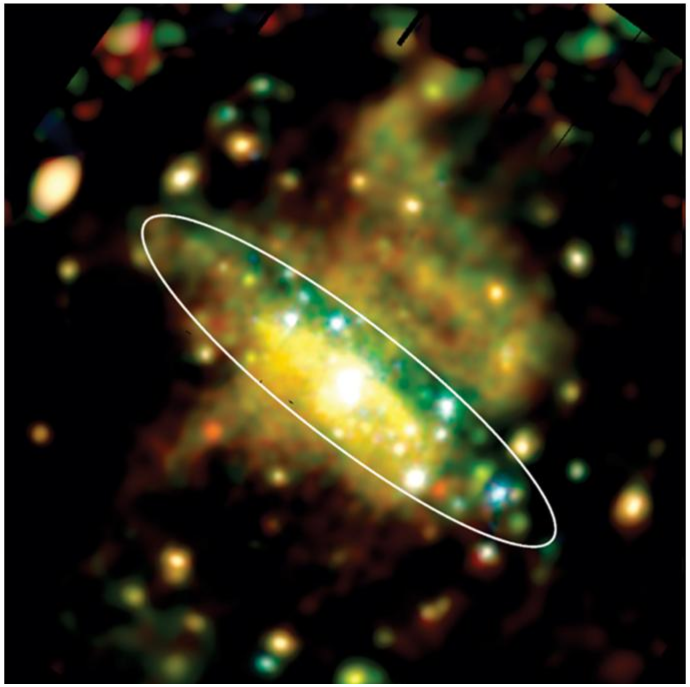

NGC 253

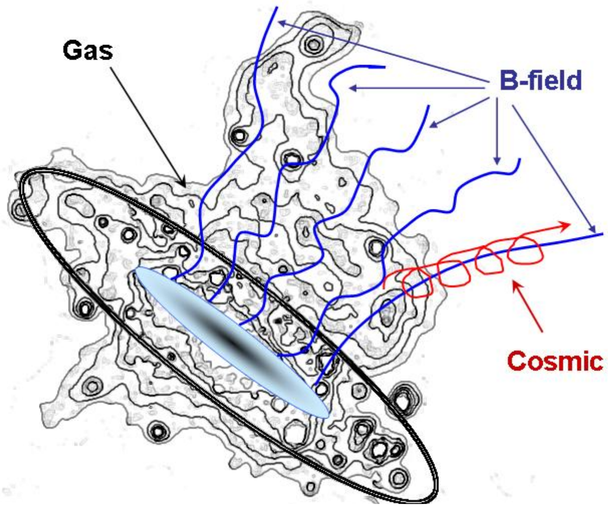

NGC 253 detected by Fermi

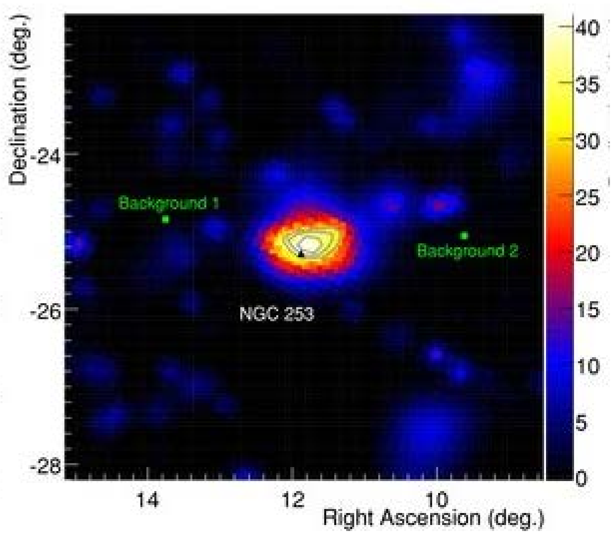

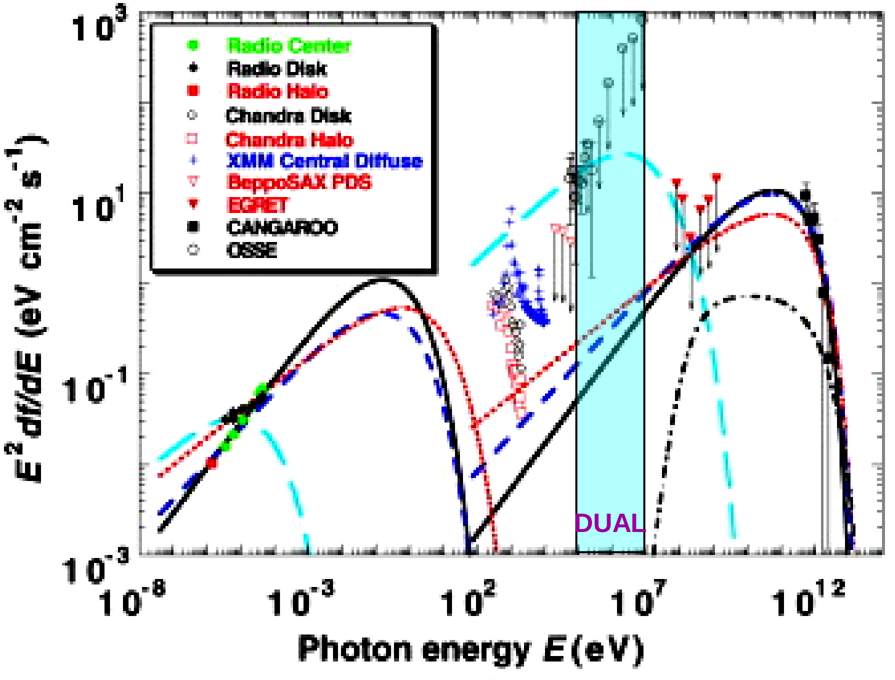

Galaxy cores

Galactic bubbles: Planck

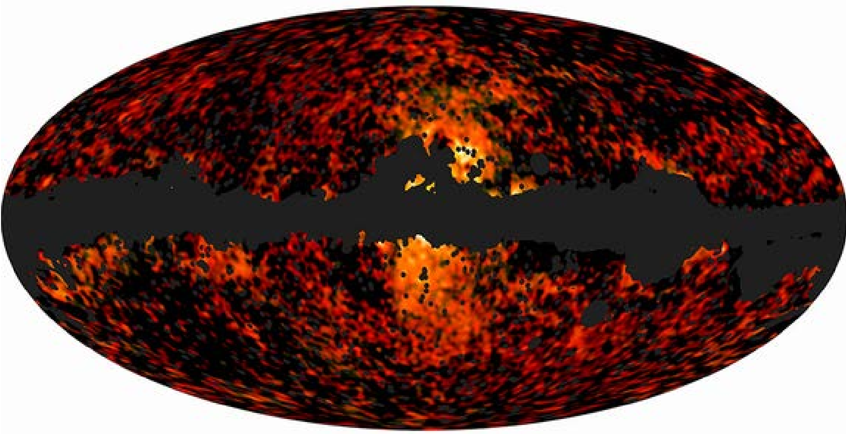

Galactic bubbles:
Planck (red) + Fermi)violet)

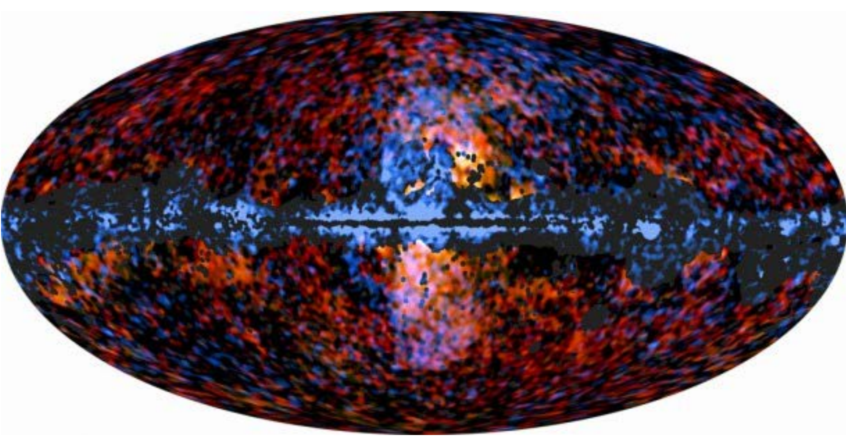

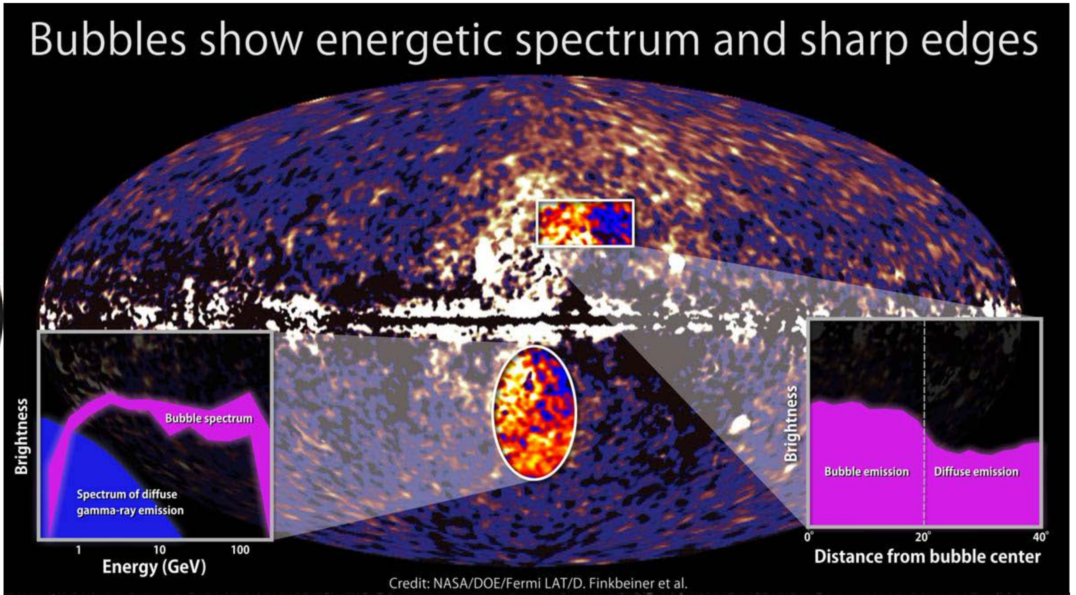

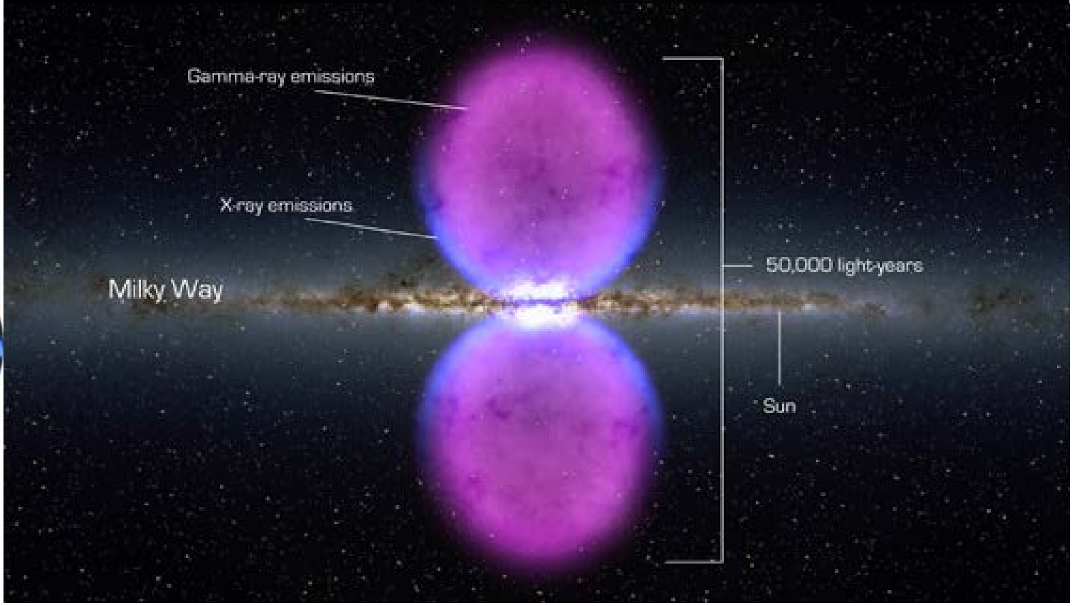

CMB photon interactions

Basic mechanisms involving CMB photons

- **γ-e: Inverse Compton Scattering**
  - Galaxy clusters
  - Radiogalaxy lobes
  - Galaxy halos

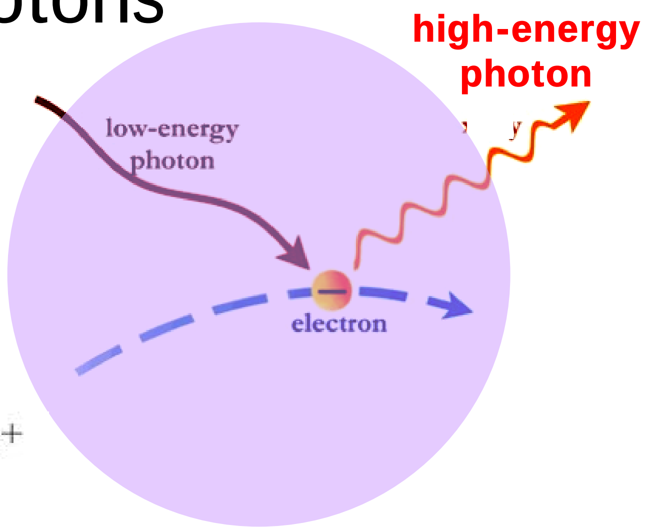

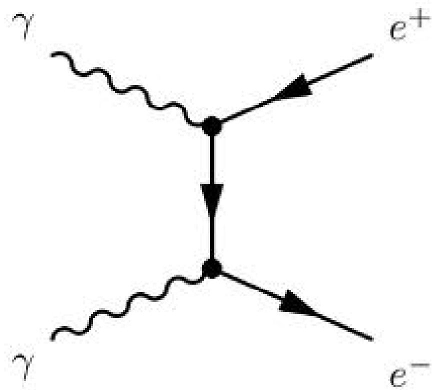

- **γ-γ: Pair production**
  - AGN jets
  - Galaxy clusters

- **γ-B: Primakov effect**
  - AGN jets
  - Galaxy clusters

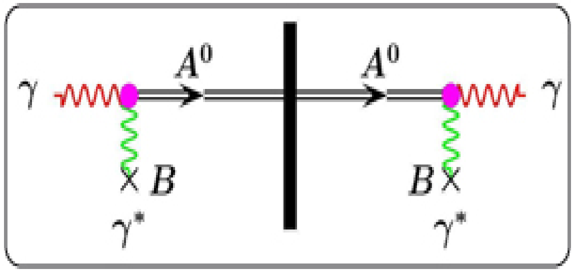

ICS

Comptonisation is a vast subject.
Inverse Compton scattering involves the scattering of low-E photons to high-E by more energetic electrons so that the photons gain and the electrons lose energy. The process is called inverse because the electrons lose energy rather than the photons, the opposite of the standard Compton effect.
We will treat the case in which the energy of the photon in the centre of momentum frame of the interaction is much less that $m_e c^2$, and consequently the Thomson scattering cross-section can be used to describe the probability of scattering.

References

Many of the most important results can be worked out using simple physical arguments, as for example in: Blumenthal and Gould (1970)
Rybicki and Lightman (1979)
Longair (1993).

ICS: a primer

IC Power From a Single Electron

Consider non-relativistic Thomson scattering in the rest frame of an electron.
If the Poynting flux (power per unit area) of a plane wave incident on the electron is

$$\vec{S} = \frac{c}{4\pi}\vec{E} \times \vec{H} = \frac{c}{4\pi}|\vec{E}|^2$$

The scattering of photon by electron at rest

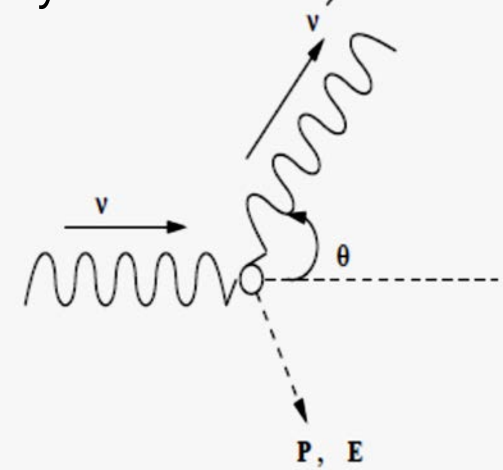

the electric field of the incident radiation will accelerate the electron, and the accelerated electron will in turn emit radiation according to Larmor's equation. The net result is simply to scatter a portion of the incoming radiation with no net transfer of energy between the radiation and the electron.
The scattered radiation has power

$$P = |\vec{S}|\sigma_T$$

where

$$\sigma_T \equiv \frac{8\pi}{3}\left(\frac{e^2}{m_e c^2}\right)^2 \approx 6.65 \times 10^{-25}\ \mathrm{cm}^2$$

ICS: a primer

In other words, the electron will extract from the incident radiation the amount of power flowing through the area and reradiate that power over the doughnut-shaped pattern given by Larmor's equation. The scattered power can be rewritten as

$$P = \sigma_{\mathrm{T}} c U_{\mathrm{rad}}$$

$U_{\mathrm{rad}} = |\vec{S}|/c$ is the energy density of the incident radiation.

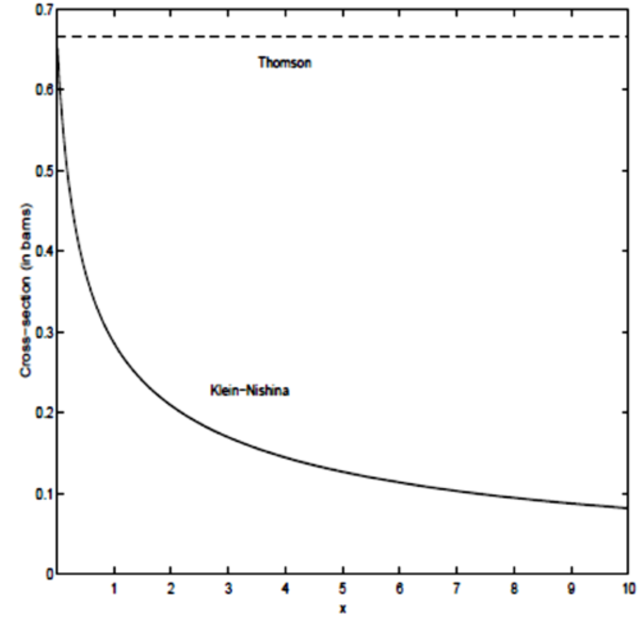

This Figure shows the plot of total cross-section for Compton scattering as a function of $x=h\nu/m_e c^2$

ICS: a primer

Reference frame transformation

Consider radiation scattering by an ultra-relativistic electron.
The Thomson scattering formula above is valid only in the primed frame instantaneously moving with the electron

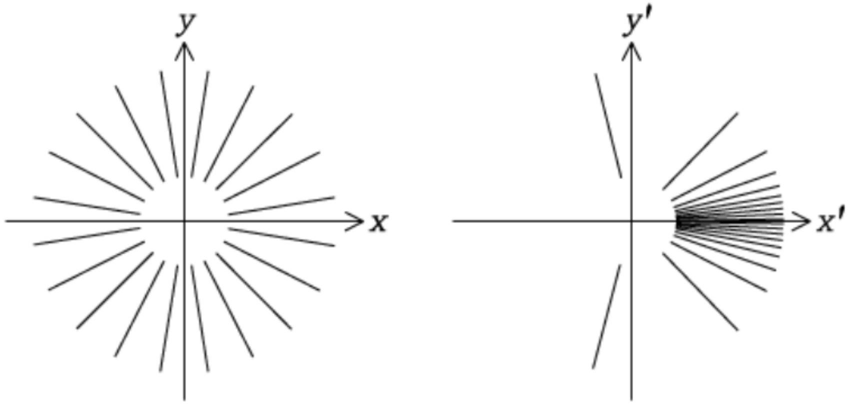

$$P' = \sigma_T c U'_{rad}$$

For a relativistic electron at rest in the "primed" frame moving with velocity v along the x axis, the angle of incidence θ' of incoming photons will be much less than the corresponding angle θ in the rest frame of the observer. This figure shows the aberration of an isotropic radiation field (left) seen in a moving frame with $\gamma = 5$ (right).

We transform this nonrelativistic result to the unprimed rest frame of an observer. It can be shown that P=P', so $P = \sigma_T c U'_{rad}$

→ We only need to transform U'_{rad} into U_{rad}

ICS: a primer

The total energy density in the electron frame of a radiation field that is isotropic in the observer's frame is obtained by integrating over all directions

$$U'_{\rm rad} = \frac{U_{\rm rad}}{4\pi}\int_{\phi=0}^{2\pi}\int_{\theta=0}^{\pi}[\gamma(1+\beta\cos\theta)]^2\sin\theta d\theta d\phi$$

Evaluating the integral yields $U'_{\rm rad} = U_{\rm rad}\left[\frac{4\gamma^2}{3} - \frac{1}{3}\gamma^2(1-\beta^2)\right]$

Recall that $\gamma^2(1-\beta^2)=1$ and then $U'_{\rm rad} = U_{\rm rad}\frac{4(\gamma^2-1/4)}{3}$

Substituting this result into $P' = P = \sigma_{\rm T} c U'_{\rm rad}$ yields

$$P = \frac{4}{3}\sigma_{\rm T} c U_{\rm rad}(\gamma^2 - 1/4)$$

This is the total power in the radiation field after ICS of low-E photons.

ICS: a primer

The initial power of these photons was $\sigma_T\, c\, U_{rad}$ so the net power added to the radiation field is

$$P_{IC} = \frac{4}{3}\sigma_T c U_{rad}(\gamma^2 - 1/4) - \sigma_T c U_{rad}$$

$$P_{IC} = \frac{4}{3}\sigma_T c U_{rad}(\gamma^2 - 1)$$

Replacing $(\gamma^2 - 1)$ by $\beta^2\gamma^2$ gives the final result

$$P_{IC} = \frac{4}{3}\sigma_T c \beta^2 \gamma^2 U_{rad}$$

for the net inverse-Compton power gained by the radiation field and lost by the electron.

When compared with the corresponding synchrotron power

$$P_{syn} = \frac{4}{3}\sigma_T c \beta^2 \gamma^2 U_B$$

there is a remarkably simple ratio of ICS to Synchrotron losses:

$$\frac{P_{IC}}{P_{syn}} = \frac{U_{rad}}{U_B}$$

ICS: a primer

The IC Spectrum of a Single Electron

Suppose the incident radiation field in the observer's frame is isotropic and composed of photons all having the same frequency ν_0, and consider scattering by a single electron moving with ultrarelativistic velocity +V along the-axis.

In the inertial frame moving with the electron, relativistic aberration causes most of the photons to approach nearly head-on.

In the observer's frame, the frequency ν of radiation scattered nearly along the +x direction is given by the relativistic Doppler formula

$$\nu = \nu'[\gamma(1+\beta\cos\theta)] \approx \nu'[\gamma(1+\beta)] \approx \nu_0[\gamma(1+\beta)]^2$$

In the ultra-relativistic regime $\beta \rightarrow 1$ one has $$\frac{\nu}{\nu_0} \approx 4\gamma^2$$

This is the maximum frequency of the upscattered radiation in the observer's frame. [Note that oblique collisions ($\theta>0$) result in lower ν]

ICS: a primer

For an isotropic radiation field in the observer's frame, the average <E> of scattered photons is equal to the average power per electron divided by the rate of photon scattering (the number of photons scattered per second by a single electron). This rate is the scattered power divided by the photon E in the observer's frame: $\rho = \frac{\sigma_T c U_{rad}}{h\nu_0}$

Thus $\langle E \rangle = h\langle \nu \rangle = \frac{P_{IC}}{\rho} = \frac{4}{3}\sigma_T c \beta^2 \gamma^2 U_{rad} \left(\frac{h\nu_0}{\sigma_T c U_{rad}} \right)^{-1}$

The average frequency <ν> of upscattered photons is: $\frac{\langle \nu \rangle}{\nu_0} = \frac{4}{3}\gamma^2$

Since $\nu_{max} = 3 \langle \nu \rangle$
it is clear that the ICS spectrum must be sharply peaked near <ν>
(see detailed calculations)

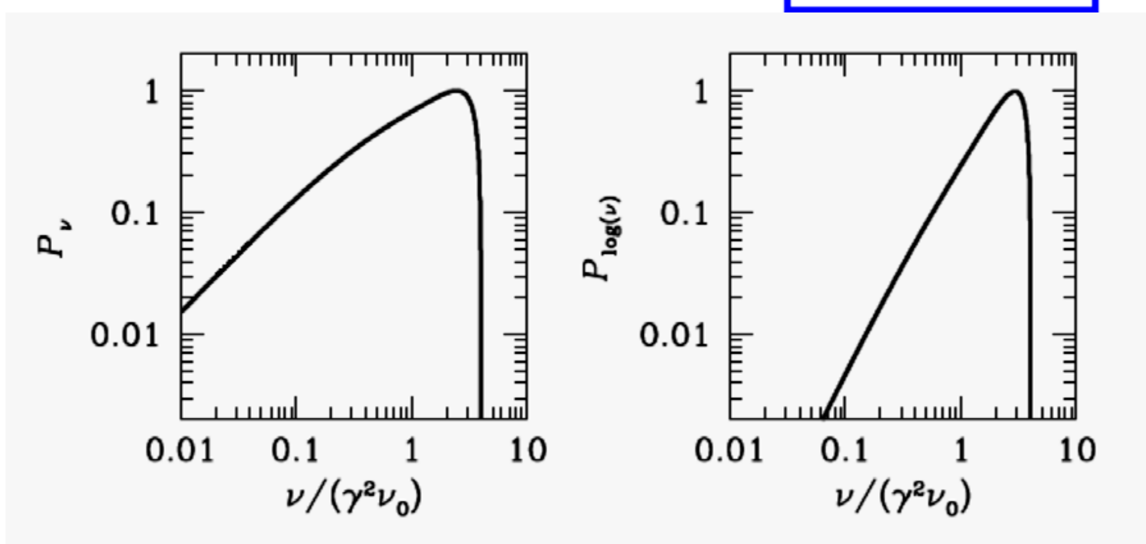

ICS: a primer

Thermal Comptonization

When $v \ll c$, $\gamma = 1$ and for a thermal distribution of non-relativistic electrons, $m_e v^2 = 3k_B T_e$, the Eq. (33) can be written as,

$$\left\langle \frac{\Delta E_\gamma}{E_\gamma} \right\rangle = \frac{4k_B T_e}{m_e c^2}. \tag{34}$$

Compton y parameter

Compton y-parameter gives the condition for a signicant change of energy of photon due to repeated N_s scattering.

After N_s scatterings, the energy change is by the factor

$$\frac{\epsilon'}{\epsilon} = \left(1 + \frac{4k_B T_e}{m_e c^2}\right)^{N_s} \simeq \exp\left(\frac{4k_B T_e N_s}{m_e c^2}\right) = \exp(4y) \qquad y = \frac{k_B T_e N_s}{m_e c^2}.$$

The energy gain by the photons (i.e.,Comptonization) goes on till the mean energy of the photons raises to 4kBTe.

The critical optical depth needed for this is determined by

$$\frac{\epsilon'}{\epsilon} = \left(\frac{4k_B T_e}{\hbar\omega_i}\right) = \exp\left[4\left(\frac{k_B T_e}{m_e c^2}\right)\tau^2{}_{crit}\right]$$

ICS: emission spectrum

When these formulae are used in astrophysical calculations, it is necessary to integrateover both the spectrum of the incidet radiation and the spectrum of the electron population.

General derivation: $$I(\nu, r) = n_{e(equil)}(E, r) \cdot \left(\frac{dE_e}{dt} \right)_{ICS} \cdot \left(\frac{dE_e}{d\nu} \right)$$

$$h\nu \approx 0.35 keV \left(\frac{E_e}{GeV} \right)^2$$

$$\left(\frac{dE_e}{dt} \right)_{ICS} = 2.5 \cdot 10^{-17} \frac{GeV}{s} \left(\frac{E_e}{GeV} \right)^2$$

Example: for a power law distribution of electrons $n_e \sim E^{-p}$ the intensity spectrum of the ICS radiation is

$$I_{ICS}(\nu) \propto E^{-(p-1)/2}$$

The synchrotron spectrum of the same electron distribution is

$$I_{Sync}(\nu) \propto E^{-(p-1)/2} \cdot B^{[(p-1)/2+1]}$$

Pair production

It is the creation of electron-positron pairs through photono-photon collisions.

Let us work out the threshold energy for this process.
If P_1 and P_2 are the momentum four-vectors of the photons before the collision

$$P_1 = [\varepsilon_1/c^2, (\varepsilon_1/c)i_1] \quad ; \quad P_2 = [\varepsilon_2/c^2, (\varepsilon_2/c)i_2], \tag{36}$$

then conservation of four-momentum requires

$$P_1 + P_2 = P_3 + P_4 \tag{37}$$

where P_3 and P_4 are the four-vectors of the created particles. To find the threshold for pair production, we require that the particles be created at rest and therefore

$$P_3 = [0, m_e] \quad ; \quad P_4 = [0, m_e]. \tag{38}$$

Squaring both sides of (37) and noting that $P_1 \cdot P_1 = P_2 \cdot P_2 = 0$ and that $P_3 \cdot P_3 = P_4 \cdot P_4 = P_3 \cdot P_4 = m_e^2 c^2$,

Pair production

$$P_1 \cdot P_1 + 2P_1 \cdot P_2 + P_2 \cdot P_2 = P_3 \cdot P_3 + 2P_3 \cdot P_4 + P_4 \cdot P_4, \quad (39)$$

$$2\left(\frac{\varepsilon_1 \varepsilon_2}{c^2} - \frac{\varepsilon_1 \varepsilon_2}{c^2}\cos\theta\right) = 4m_e^2 c^2, \quad (40)$$

$$\varepsilon_2 = \frac{2m_e^2 c^4}{\varepsilon_1(1-\cos\theta)}, \quad (41)$$

where θ is the angle between the incident directions of the photons. Thus, if electron-positron pairs are created, the threshold for the process occurs for head-on collisions, $\theta = \pi$ and hence,

$$\varepsilon_2 \geq \frac{m_e^2 c^4}{\varepsilon_1} = \frac{0.26 \times 10^{12}}{\varepsilon_1}\,\mathrm{eV}, \quad (42)$$

where ε_1 is measured in electron volts. This process thus provides not only a means for creating electron-positron pairs, but also results an *important source of opacity* for very-high-energy γ-rays.

Pair production

The table shows some important examples of combinations of ε_1 and ε_2. Photons with energies greater than those in the last column are expected to suffer some degree of absorption when they traverse regions with high energy densities of photons with energies listed in the first column.

	ε_1(eV)	ε_1(eV)
Microwave Background Radiation	6×10^{-4}	4×10^{14}
Starlight	2	10^{11}
X-ray	10^3	3×10^8

The cross-section for this process for head-on colisions in the ultrarelativistic limit is

$$\sigma = \pi r_e^2 \frac{m_e^2 c^4}{\varepsilon_1 \varepsilon_2} \left[2 \ln \left(\frac{2\omega}{m_e c^2} \right) - 1 \right] \qquad (43)$$

where $\omega = (\varepsilon_1 \varepsilon_2)^{1/2}$ and r_e is the classical electron radius.

Pair production

In the limit $\hbar\omega \approx m_e c^2$, the cross-section is

$$\sigma = \pi r_e^2 \left(1 - \frac{m_e^2 c^4}{\omega^2}\right)^{1/2} \tag{44}$$

Thus, near threshold, the cross-section for the interaction $\gamma\gamma \rightarrow e^+e^-$ is

$$\sigma \sim \pi r_e^2 \sim 0.2\sigma_T. \tag{45}$$

These cross-sections enable the opacity of the interstellar and intergalactic medium to be evaluated as well as providing a mechanism by which large fluxes of positrons could be generated in the vicinity of active galactic nuclei. These results are very important for the ultra-high γ-ray emission detected by instruments such as the HESS array in Namibia.

Primakov effect

Axion-photon coupling:

$$\mathcal{L}_{A\gamma\gamma} = -g_\gamma \frac{\alpha}{\pi} \frac{A(x)}{f_A} \vec{E} \cdot \vec{B}$$

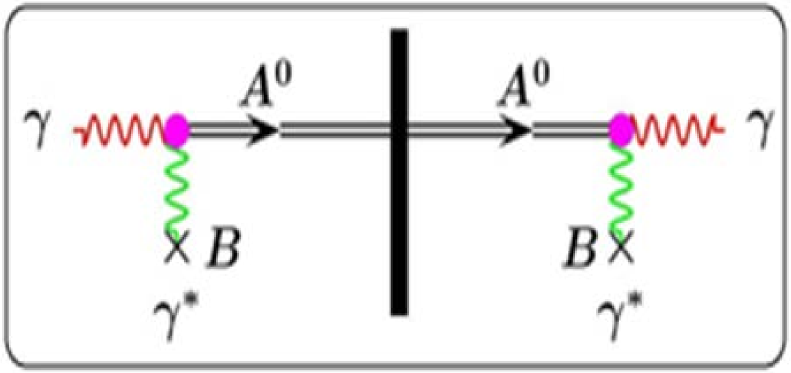

This can lead to the conversion of an axion to a photon in a magnetic field, or vice versa

Dark Matter

- For $m_A = 10^{-5}$eV at 2.7 K = 2×10^{-4} eV
- These "thermal" axions would be relativistic

Further readings

Colafrancesco: 2010MmSAI..81..104C
: 2008ChJAS...8...61C
: 2008MmSAI..79..213C
: 2010AIPC.1206....5C
Blumenthal and Gould (1970): 1970RvMP...42..237B
Rybicki and Lightman (1979): Radiative Processes in Astrophysics
Longair (1993): High Energy Asrophysics